

A. Bioimpedance monitoring for physicians: an overview ¹

Sometimes I have had to explain the basics of electrical Bioimpedance Monitoring (BM) to physicians, biologists or veterinarians, all of them from the biomedical community and familiarized with cell biology. In general, those professionals are not skilled in circuit theory or electromagnetism and I found difficulties to explain concepts such as impedance phase, real part of the impedance, complex numbers... In these cases, I would have liked to provide them some written material to clarify those concepts. Unfortunately, the literature about bioimpedance is mostly written by physicists for physicists and a background in electromagnetic theory is assumed. On the other hand, the basic circuit theory texts are too much dense and remote from the bioimpedance field. Therefore, I thought that a short paper trying to fill this gap could be profitable.

I have not tried to write a scientific review about BM. The objective has been to be didactic and, because of that, I have specially focused on the electrical concepts.

¹ I originally wrote this paper as an exercise to obtain the diploma from the course “Medicina per a no metges” (Medicine for non physicians, October 2001 – July 2002) held at Hospital Clínic de Barcelona.

A.1. Introduction

Electrical Bioimpedance Monitoring is an emerging tool for biomedical research and for medical practice. It constitutes one of the diagnostic methods based on the study of the passive electrical properties² of the biological tissues. These properties have been object of study since Luigi Galvani (1737-1789) discovered that while an assistant was touching the sciatic nerve of a frog with a metal scalpel, the frog's muscle moved when he drew electric arcs on a nearby electrostatic machine. However, it was not until the end of XIX [1] that these properties started to be measured thanks to the development of new instrumentation and the set up of the electromagnetic field theory by James Clerk Maxwell (1831-1879).

The practical use of the electrical passive properties started in the middle of the XX century. Different properties and techniques resulted in a collection of methods that are now used for multiple applications. Usually, these methods have three advantages in common:

- require low-cost instrumentation.
- are easily applicable in practice.
- enable on-line monitoring.

Excellent reviews about the applications of Bioimpedance (BI) methods can be found in [2-4]. Here some of these applications are listed in order to show the BI potentiality.

A.1.1. Cellular Measurements

Coulter counter. This method is the best known application of impedance methods in the cellular field. It is used to count the amount of cells in a suspension. The measuring principle is quite simple: cells are forced, or enabled, to pass through a capillary (~100 μm) that changes its electrical impedance at each cell passage. Then, the concentration of cells is estimated from the rate of impedance fluctuations and, in some cases, it is even possible to extract information about the cell sizes from the impedance peak values at each cell passage.

Measurement of the hematocrit. The concentration of dielectric particles in a conductive solution can be estimated if the shape and size of the particles is known. This fact has been used in commercial blood analyzers to determine the hematocrit.

² The passive electrical properties are determined by the observation of the tissue electrical response to the injection of external electrical energy. That is, the tissue is characterized as it was an electrical circuit composed by resistors, capacitors, inductors...

Some biological tissues also show active electrical properties since they are capable of generating currents and voltages (e.g. the nerves).

Monitoring of cell cultures. BI can be used to quantify the biomass in industrial bioreactors [5;6] or to study the response of cellular cultures to external agents (toxins, drugs, high-voltage shocks and electroporation) [7;8].

A.1.2. Volume Changes

As it will be explained later, the bioimpedance is not only related with the tissue properties but it also depends on the geometrical dimensions. Therefore, it is possible to measure sizes or volumes when some data about the tissue electrical conductive properties is known a priori. Moreover, if tissue electrical properties remain constant, it is possible to obtain information about volume or size changes from the detected impedance fluctuations [9].

Impedance plethysmography. In this method BI is used to estimate the blood volume in the extremities. One of its applications is the detection of venous thromboses and stenoses in the extremities by measuring the blood filling time when an occlusion of the veins in the limb is removed.

Impedance cardiography. The stroke volume of the heart can be estimated by measuring impedance via an invasive mutielectrode catheter or with skin electrodes (transthoracic impedance cardiography.)

Impedance pneumography. The same principles of the impedance cardiography can be also applied for monitoring the respiration air volumes.

A.1.3. Body composition

As the BI depends on the tissue properties and on its geometry, it is possible to estimate the relative volumes of different tissues or fluids in the body.

Fluid compartments. For the determination of the total body water, the relative volumes of extra and intracellular spaces are estimated by measuring BI. Two procedures are in use: bioimpedance analysis (BIA) and bioimpedance spectroscopy (BIS). BIA measures impedance at a single frequency and assumes that the measured value corresponds to the extracellular fluid volume. However, the broad variety of persons and pathologies causes important disturbances. Those disturbances are reduced when BIS (measurement at several frequencies) is applied.

Fat compartments. With important restrictions, the same techniques of the hydration monitoring can be applied to calculate the fat/fat-free mass volumes.

A.1.4. Tissue classification

Since different tissue types exhibit different conductivity parameters, it is easy to conceive that BI can be applied to characterize the tissues. Obviously, the most interesting application would be the cancer detection. Unfortunately, although this idea was born long ago few significant achievements have been obtained up to now and the field is still under research [10-12].

Nevertheless, it must be said that one multichannel-BIS device is now commercially available for breast cancer screening (TranScan TS2000, TransScan Medical Ltd., Israel). The probe consists of an array of electrodes that is pressed onto the breast. The system displays a map of the impedance which yields typical patterns for healthy and cancerous breast. Its sensitivity for the verification of suspicious breast lesions has been positively demonstrated although its clinical usage could be limited by a high false positive rate [13].

A.1.5. Tissue Monitoring

Cellular edema, interstitial edema and gap junctions closure are some events that induce variations of the BI parameters. These events are related to the metabolism of the tissue cells and their on-line monitoring could be of great relevance. Nowadays, this field of application is at the research level. However, the results are very promising and a future clinical usage seems reasonable.

Ischemia monitoring. In some cardiac surgical procedures the heart is artificially arrested. In these cases, the medical team does not have any information about the myocardium condition and the unique controllable parameter is the time before circulation is restored (ischemia period). Thus, a system able to indicate the evolution of the damage caused to the heart by the ischemia is interesting [14]. Several papers show that ischemia in the heart, and in other organs or tissues, imply the alteration of some BI parameters [13;15-26].

Graft viability assessment. BI monitoring of organs to be transplanted has been proposed to determine which organs are suitable for transplantation. The idea is to quantify the damage caused by ischemia before, during and after the transplantation [27-37].

Graft rejection monitoring. The rejection processes in transplanted organs cause inflammatory processes that could be detected by BI measurements [38;39]. An implanted electrode probe with telemetry has been proposed for this application [34].

Glucose monitoring. Quite recently it has been proposed a non-invasive continuous glucose monitoring system based on impedance spectroscopy [40].

A.1.6. Electrical Impedance Tomography

Electrical impedance Tomography (EIT) expands the usefulness of all these methods by adding spatial resolution. EIT provides a mapping of the impedance distribution in a tissue layer or volume. Multiple electrodes are used to inject and record the voltages and currents and computer reconstruction algorithms process the resulting data to generate an image. The resolution is very poor compared to other imaging methods (echography, X-ray tomography or Magnetic Nuclear Resonance) but it is sometimes justified in terms of cost, acquisition speed and information provided by the quantitative results. However, although some clinical studies have been carried out, EIT is not applied now as a standardized method. For more information about EIT read [3].

A.2. Circuit theory

Impedance is a common word in electronics. It denotes the relation between the voltage and the current in a component or system. Usually, it is simply described as the **opposition** to the flow of an alternating electric current through a conductor. However, impedance is a broader concept that includes the **phase shift** between the voltage and the current. We will see it later, but first it is necessary to review some basic concepts about electricity.

Voltage (or potential) in a point A indicates the energy of an unitary charge located in this point compared to the energy of an unitary charge in a point B. If an electric path exists, this energy difference forces the electronic charges to move from the high energy position to the low energy position. In other words, voltage is the electrical force that causes current to flow in a circuit. Voltage is measured in Volts (V).

Traditionally, an analogy with water pressure has been set up in order to explain the voltage concept.

The **electrical current** denotes the flow of electrical charge (Q) through a cross-section in a second. It is measured in Amperes (A) (= Coulombs/s.m²).

Following the same hydraulic analogy, current is viewed as the water flow (amount of liters/second) through a pipe.

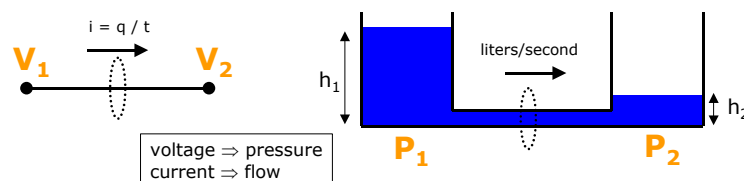


Figure A. 1. Electrical current and voltage to water flow and pressure analogies.

Charge can exist in nature with either positive or negative polarity. Forces of attraction exist between opposite charges and forces of repulsion exist between like charges.

In materials that conduct electricity, some particles exist that are able to move. These particles are called **charge carriers** and they are usually **electrons** or **ions**. There are many materials, called insulators or dielectrics, that do not conduct electricity. All the charges in these materials are fixed (**fixed charges**).

A.2.1. Resistive networks

In an element able to conduct electricity, such as a metal, the **resistance (R)** denotes the relation between the applied voltage difference and the flowing current. It is measured in Ohms (Ω). The resistance of an ideal conductor (superconductor) is 0Ω whereas the resistance of an ideal dielectric is infinite.

The **Ohm's law** says that there exist a linear relation between voltage and current:

$$v=i.R$$

This law is valid for most materials but there are some exceptions. For instance, biological tissues do not obey Ohm's law if the current density (current/cross-section area) is beyond a threshold³.

Resistance implies energy loss. The amount of energy lost by a conductor in a second (Power) is:

$$P= v.i \quad [W= V.A]$$

The resistance is compared to the opposition of water flow in a pipe.

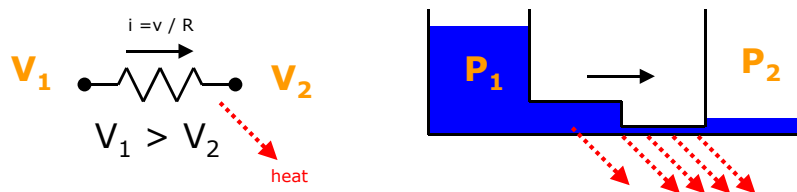


Figure A. 2. Resistance symbol and its hydraulic analogy.

³ When a system obeys the Ohm's law it is said to be a linear system because all the voltages and currents are related through linear expressions.

The resistance depends on different parameters and physical facts:

- Amount of charge carriers in the conductor. The resistance is inversely related to the concentration of charge carriers. For example, in an ionic solution the **conductance** ($=1/R$) is directly related to the ion concentration⁴.
- Mobility of the charge carriers. Charges are freer to move in some circumstances and that determines the resistance. For example, in ionic solution the 'viscosity' of the solvent decreases as the temperature rises, increasing the ion mobility and, consequently, decreasing the resistance. On the contrary, in metals, electronic conductors, the temperature causes electrons to collide more frequently and that causes a mobility decrease.
- Geometrical constraints. The resistance is inversely related to the conductor section and it is directly related to the conductor length. For a given material and temperature, the **resistivity** (ρ , units [$\Omega \cdot \text{cm}$]) is defined as:

$$R = \rho \times (\text{Length}/\text{Section})$$

In a circuit, the elements able to provide energy are:

Voltage source. An element that maintains a fixed voltage difference between its two terminals no matter the current that is flowing through it. This element would be analogous to a waterfall. The most known examples are batteries.



Figure A. 3. Voltage source symbols.

Current source. An element that maintains a fixed current through it no matter the voltage difference between its terminals. This element would be analogous to a peristaltic pump.

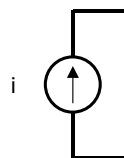


Figure A. 4. Current source symbol.

⁴ This is true if the concentration is not too much high.

An electric circuit containing multiple connected resistors⁵ can be modeled as a single resistance. That is, the circuit behaves as a single resistance. The following examples show how this simplification is performed.

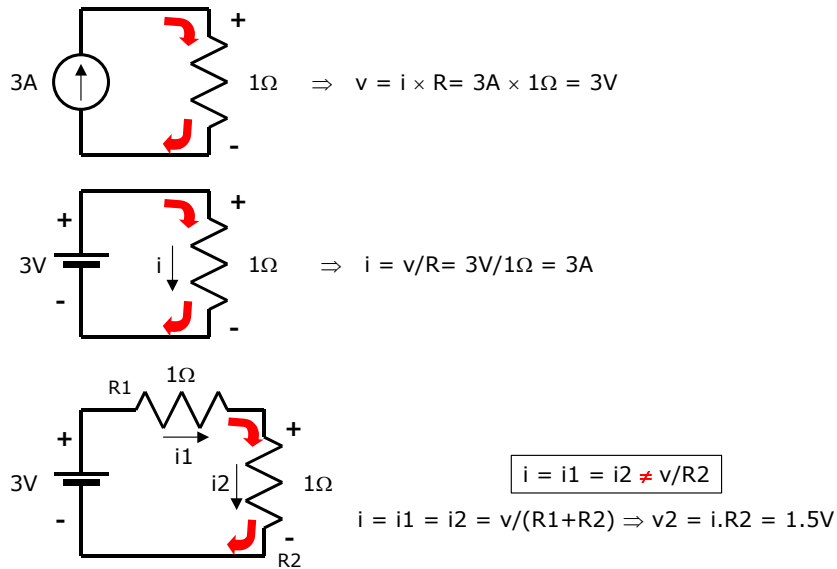


Figure A. 5. Simple circuit examples.

Resistors in series:

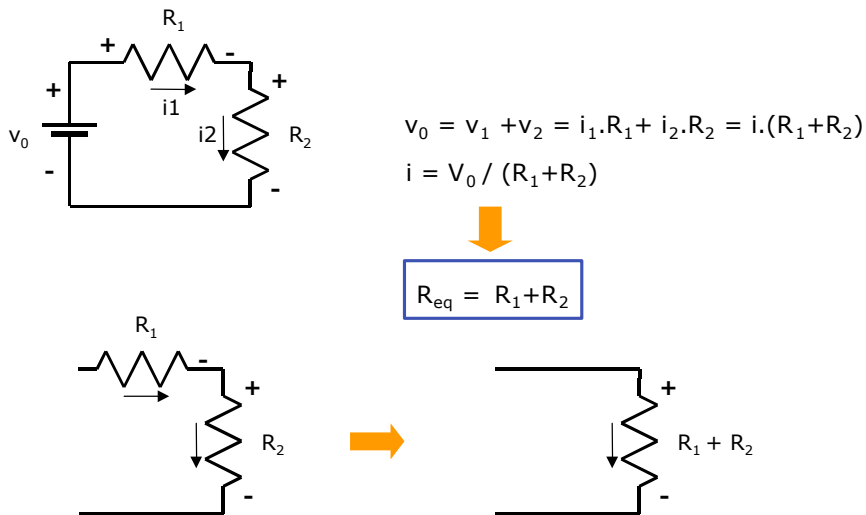


Figure A. 6. Equivalent resistance for two resistances in series.

⁵ A resistor is an electric component with a fixed resistance.

Resistors in parallel:

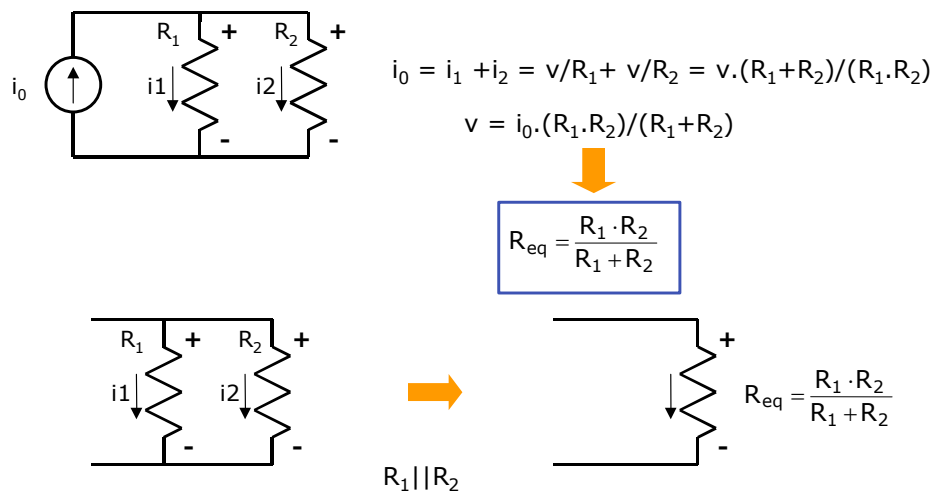


Figure A. 7. Equivalent resistance for two resistances in parallel.

In a biological tissue, each slab of extra-cellular space can be modeled as a resistance. Thus, as we have seen, the behavior of the whole extracellular space could be modeled by a single resistance. Unfortunately, biological tissues are more complex than that, they include dielectrics and consequently they show time dependent responses.

A.2.2. Time and frequency response in linear systems

Apart from fixed value voltage and current sources, it is also possible to find, or to implement, sources with a time dependent output. Here, two examples are presented.

Step voltage source:

The output voltage is 0 V until time equals t_0 . Then, the voltage is A.



Figure A. 8. Step voltage source symbol and its time-dependent response.

Sinusoidal voltage source:

The output voltage is a time dependent sinusoid⁶. The shape of the sinusoid is determined by the frequency (number of cycles/second), by the amplitude (maximum voltage value) and by the so called phase angle or phase (expressed in degrees).

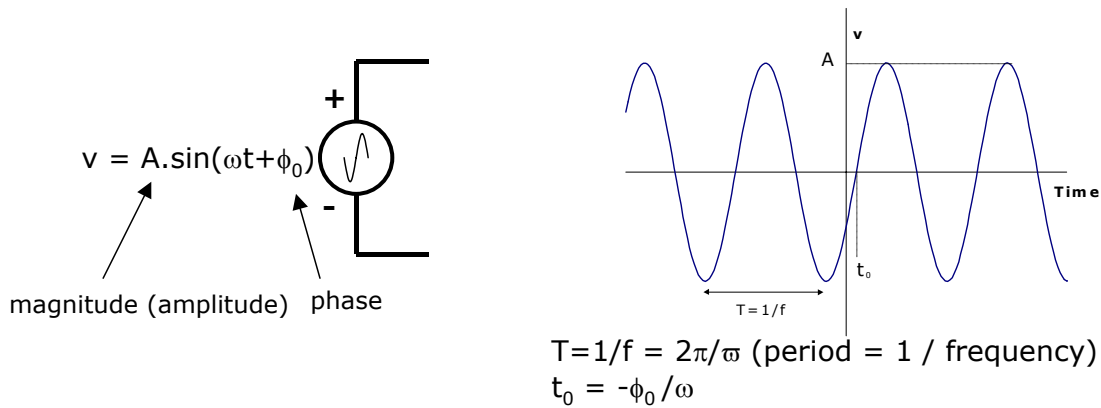


Figure A. 9. Sinusoidal voltage source symbol, equation and its time-dependent response.

The phase determines when the sinusoid starts. It can be understood as a delay (t_0) and its value can be either positive or negative.

As it has been said, the biological tissues include dielectrics. Apart from the fact that the resistance of these materials is ideally infinite, they imply another electrical phenomenon: **capacitance**.

Dielectrics are not capable to conduct charge but they are capable to store it. The basic charge accumulator is the **parallel-plate structure**. This element consists of two conductive plates separated by a dielectric. The amount of charge that it is capable to store (Q) is determined by its dimensions and by a dielectric parameter: **permittivity** ($\epsilon = \epsilon_r \cdot \epsilon_0$). The **capacitance** (C) relates the voltage with the accumulated charge and it is measured in Farads [F]

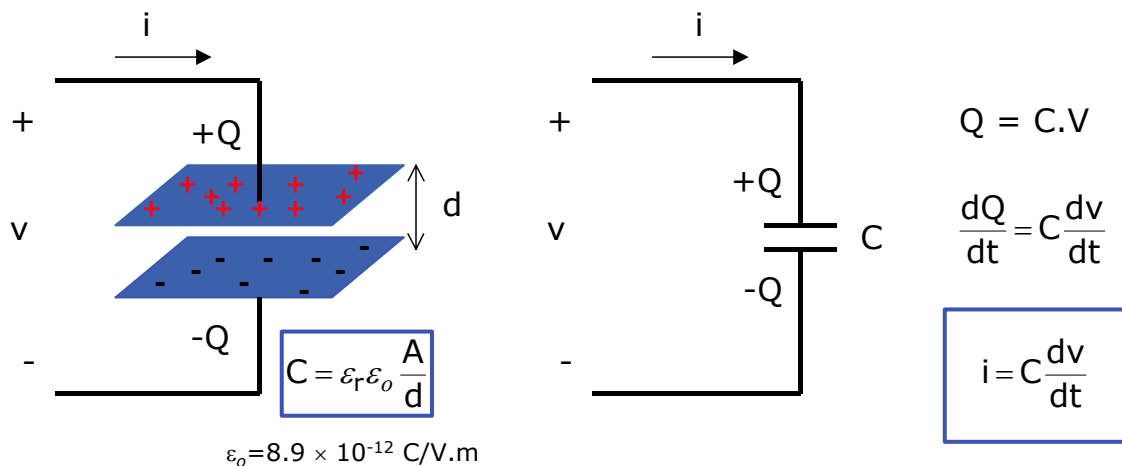


Figure A. 10. Schematic representation of the parallel-plate structure and the main equations related with the capacitance phenomenon.

⁶ This signals are also referred as **AC signals** (AC = alternating current).

The relative permittivity (ϵ_r) depends on the material between the two plates. If this material is vacuum or air, the permittivity equals ϵ_0 ($\epsilon_r = 1$).

From the equations it can be easily observed that the relation between voltage and current depends on time. If the capacitance voltage is kept constant, no current enters or leaves the capacitance. However, if this voltage changes with time, a certain quantity of current (proportional to the time derivative of the voltage) will enter and leave the capacitance to charge or to discharge it. That does not mean that charge carriers can physically flow through the dielectric but, from the voltage source point of view that is what happens when the voltage is not constant with time. That is, if a time varying voltage is applied to the capacitance, some current is able to flow through the source.

The following example shows what happens when a pulse-train voltage source is connected to a circuit composed by a resistance and a capacitance (RC circuit).

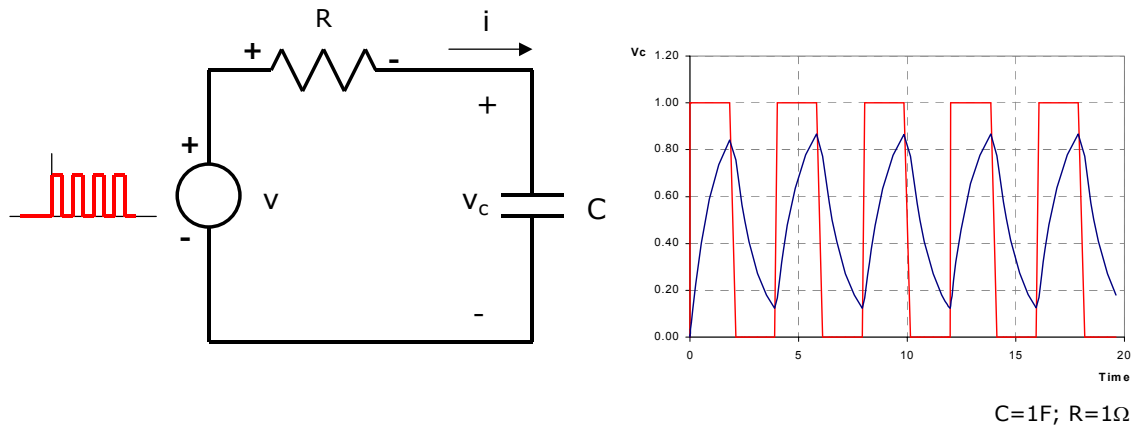


Figure A. 11. RC circuit and its response to a pulse-train. The input voltage is plotted in red and the capacitance voltage is plotted in blue.

At the beginning the capacitance is discharged ($Q=0$ Coulombs) and, consequently, the voltage difference between its terminals is 0 V. The first input voltage pulse (plotted in red) causes some current to flow through the resistance and starts to charge the capacitance. However, since the capacitance increases its voltage (plotted in blue), the current decreases and the voltage evolution is flattened.

When the voltage source comes back to 0 V, the capacitance is charged and it starts to return the accumulated charge through the resistance. The evolution is also flattened because the capacitance voltage decreases as it loses charge.

As it can be observed, for this kind of input signal, the voltages and currents in the circuit can show a different shape (input: rectangular pulse train \rightarrow output: saw shape). However, there is a special kind of signal that maintains its shape: the sinusoidal signal.

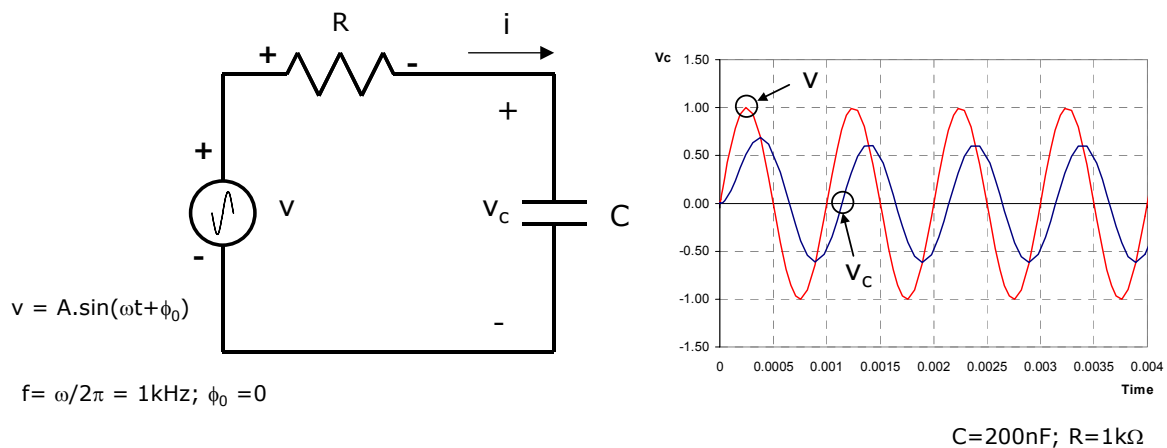


Figure A. 12. RC circuit and its response to a sinusoidal signal.

The voltage at the capacitor is a sinusoidal with the same frequency as the voltage source. The only differences are the amplitude and the phase. The same can be said about all the voltages and currents around the circuit. This is a fundamental property of linear circuits (for instance, any combination of resistors, capacitors and inductors):

In a linear circuit, when the excitatory signal is a sinusoidal current or voltage source, all voltages and currents are sinusoidal signals with the same frequency of the excitatory signal.

This fact, combined with the fact that any signal can be expressed as a combination of sinusoids (Fourier Series) is of great relevance in electronics and communications. Once that the circuit has been characterized for each frequency (two parameters for each frequency: amplitude and delay) it is possible to compute the output signal for any kind of input signal.

The **impedance** of an element at a certain frequency is defined as the relation between the input voltage and the input current for that frequency. Thus, it should be clear that for a linear element two relations will exist between voltage and current: 1) relation of amplitudes (or modulus or magnitudes) and 2) relation phases ('delay' between current and voltage).

AC signals are usually represented as **complex numbers**. This special kind of numbers contains information of the modulus and the phase. Below there are some figures and equations trying to explain this concept. However, the only thing that must be clearly understood is that complex numbers are a proper way to represent modulus and phase simultaneously. The reason to use this nomenclature is for calculus.

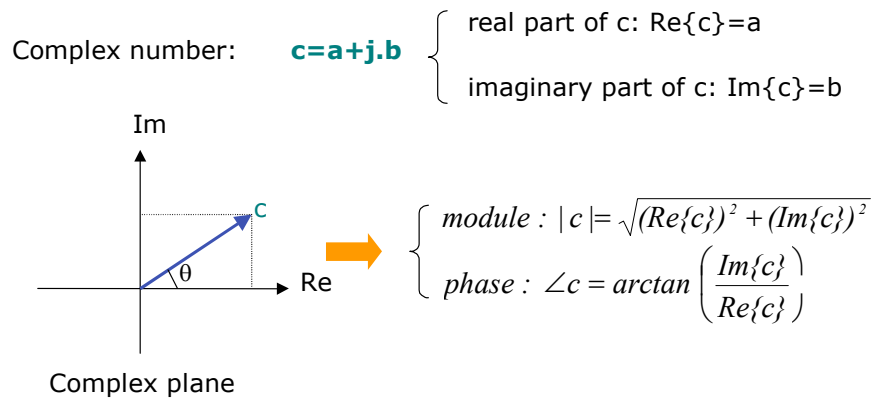


Figure A. 13. Graphical representation of a complex number on the complex plane and the relationships between the two possible ways to describe a complex number.

In electronics, the letter j ($\sqrt{-1} = (-1)^{1/2}$) is used instead of i to avoid confusions with the current symbol.

A.2.3. Electrical impedance

For a given frequency, if \mathbf{V} and \mathbf{I} are the complex numbers that represent the input voltage and current (magnitude and phase): The **electrical impedance**, \mathbf{Z} , is a complex number with magnitude equal to the relation of magnitudes and phase equal to the difference of phases.

$$\mathbf{Z} = \mathbf{V} / \mathbf{I} \Rightarrow \left\{ \begin{array}{l} |\mathbf{Z}| = |\mathbf{V}| / |\mathbf{I}| \\ \angle \mathbf{Z} = \angle \mathbf{V} - \angle \mathbf{I} \end{array} \right.$$

The real part of the impedance is called **resistance** while the imaginary part is called **reactance**. The resistive part causes the power loss (the impedance of a resistor is purely resistive, without reactance term, $\mathbf{Z} = \operatorname{Re}\{\mathbf{Z}\}$) whereas the reactance causes the delay between voltage and current (the impedance of a capacitor is purely reactive $\mathbf{Z} = j \cdot \operatorname{Im}\{\mathbf{Z}\}$).

Although it is not strictly accurate, the impedance concept is also applied when voltage and currents are injected or measured at different points. In those cases it would be more correct to use the term **transimpedance**.

Impedance of a resistance:

As it has been shown before, a resistance obeys the Ohm's law per definition. Thus, the only relation between voltage and current can be a relation of magnitudes.

$$Z = \text{Re} \{Z\} = R = V/I$$

The same expression is valid for any combination of resistances that can be grouped as a single equivalent resistance.

Impedance of a capacitance:

For a capacitance, the current is proportional to the time derivative of voltage. This means that the Ohm's law as we expressed before is no longer valid.

The impedance of a capacitance is ⁷:

$$Z = -j \cdot (1/(2 \cdot \pi \cdot f \cdot C))$$

Thus, the capacitance impedance depends on frequency (f) and is purely reactive (phase angle = -90°).

It is sometimes said that a capacitance behaves as a resistance with value $1/2\pi fC$: an open-circuit (no conductance) for very low frequencies and a short-circuit for high frequencies. Another way to say the same:

In a capacitance, high frequency currents are free to flow and low frequency currents are blocked.

This rule is especially useful to understand intuitively the behavior of simple RC circuits.

Extended Ohm's law:

The Ohm's law, and the parallel and series equivalents, can be applied to any linear circuit using the impedance complex values. For instance, the following figure shows how to calculate the impedance of a circuit formed by a resistance and a capacitance in series.

⁷ The demonstration of this expression is beyond the scope of this paper.

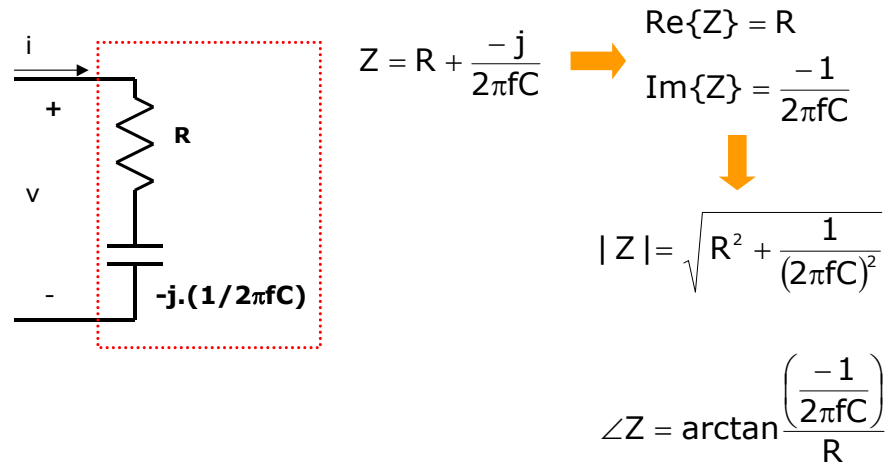


Figure A. 14. Impedance calculus of a simple RC circuit.

For $R = 1 \text{ k}\Omega$ and $C = 100 \text{ nF}$ (10^{-9} F) the following graphs are obtained:

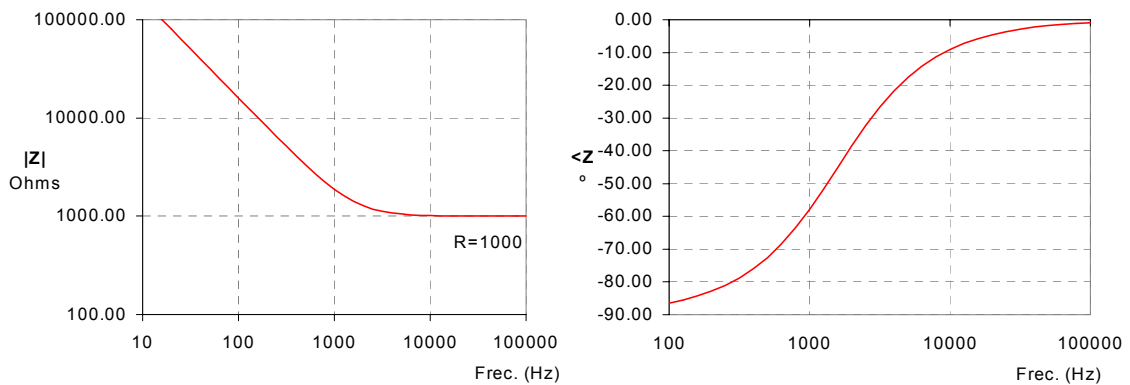


Figure A. 15. Bode plots of the impedance.

These graphs are the **Bode plots** of the impedance. On the left, the magnitude, or modulus, of the impedance is displayed for each frequency (f). Both axes, horizontal and vertical, are expressed in logarithm base 10. The graph on the right shows the phase value for each frequency. In this case, only the frequency is expressed in the logarithm form.

It is possible to describe intuitively such behavior. At low frequencies, $f < 10 \text{ Hz}$, the capacitance blocks the current and, therefore, the impedance modulus must be very high. Because of that, the 'most important' impedance is the impedance of the capacitance and the phase is imposed by it. Thus, the impedance phase gets closer to -90° as the frequency is reduced. On the other side, at high frequencies, the current is free to flow through the capacitance and the limiting element is the resistance.

In the following example, try to describe the Bode graphs by yourself ($C=100\text{nF}$, $R_1=1\text{k}\Omega$ and $R_2=1\text{k}\Omega$):

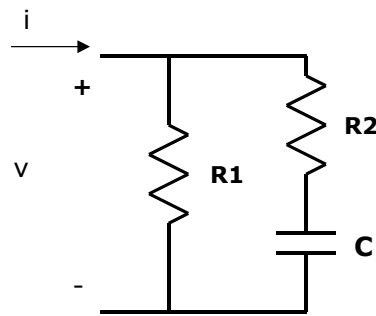


Figure A. 16. Circuit composed by a resistance in parallel with the series combination of a resistance and a capacitance.

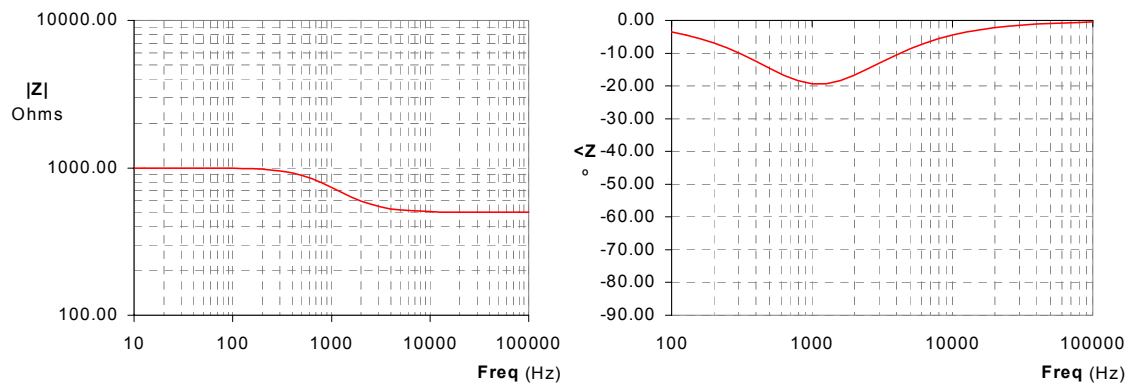


Figure A. 17. Bode plots of the impedance of the circuit depicted in Figure A. 16.

At low frequencies the current is blocked by the capacitance and the current is only capable to flow through $R1$. Therefore, the impedance is imposed by $R1$ and that means that the modulus is $|R1| = R1 = 1 \text{ k}\Omega$ and the phase is $\angle R1 = 0^\circ$. At high frequencies the capacitance behaves as a short-circuit and the impedance is $R1$ in parallel with $R2 = R1 \parallel R2 = (R1 \cdot R2) / (R1 + R2) = 500 \Omega$. In this case it will be said that a single **dispersion** exists, that is, a single transition from a constant impedance value ($|Z|$ at low frequencies) to another constant value ($|Z|$ at high frequencies) is detected. In general, the number of observable dispersions (or transitions) will depend on the number of RC branches provided that their values are quite dissimilar (different frequency regions).

The same information can be displayed using another kind of representation: the **Wessel diagram** (also called **Cole diagram** or **Nyquist plot**).

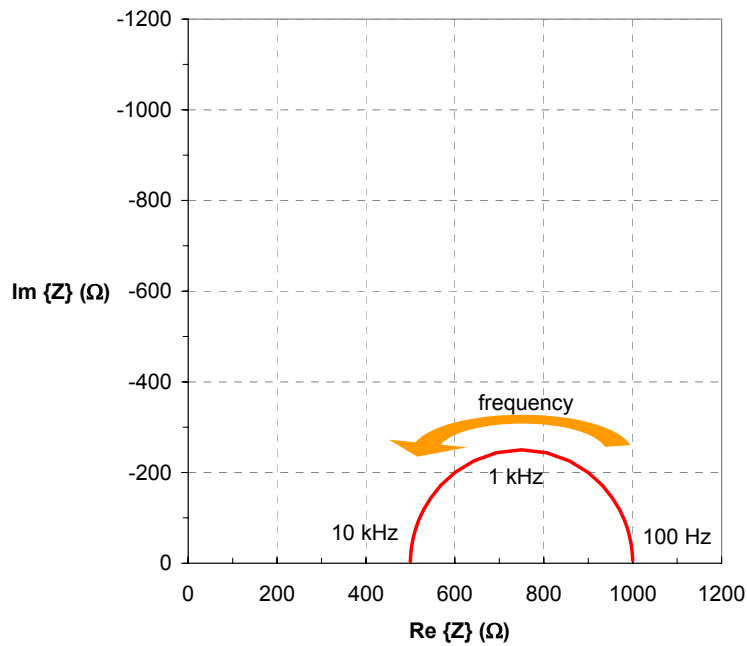


Figure A. 18. Wessel diagram (or Nyquist plot) of the impedance of the circuit depicted in Figure A. 16.

The imaginary part (with negative sign) of the impedance is plotted versus the real part of the impedance for each frequency. This representation is particularly used in electrochemistry and has been adopted by many researchers in the bioimpedance field. Its main advantage is that each dispersion is easily identified because it is displayed as an arc.

A.2.4. Electrical characterization of the materials

As it has been noted, the impedance values are not only determined by the electrical properties of the materials (conductivity and permittivity) but also by the geometrical constraints. In general, the values of interest will be the electrical properties of the materials since they will be not dependent on the geometry used in each study. The values displayed by the instrumentation setup will be expressed as impedance or conductance values but they are easily transformed into material electrical properties by applying a scaling factor that depends on the geometry, the **cell constant**. The reference geometry is a cubic slab of the material in which the impedance is measured through two ideally conducting plates at opposite sides. In the bioimpedance field, the size of this cube is usually $1\text{ cm} \times 1\text{ cm} \times 1\text{ cm}$.

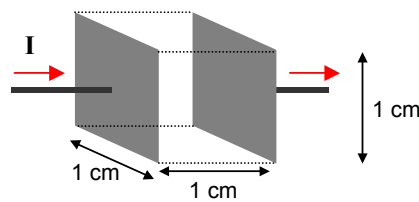


Figure A. 19. Reference measurement cell.

$$Y = G + jB = G + j\omega C = K(\sigma + j\omega\varepsilon) = K(\sigma + j\omega\varepsilon_r\varepsilon_0)$$

Where:

Y is the admittance ($=1/Z$, inverse of the impedance)

G is the real part of the admittance and it is called conductance (expressed in Siemens (S) = $1/\text{Ohm}$ ($1/\Omega$))

B is the imaginary part of the admittance and it is called susceptance (expressed in Siemens (S) = $1/\text{Ohm}$ ($1/\Omega$))

C is the capacitance (expressed in Farads (F))

K is the scaling factor of the measurement cell = area/length (expressed in $\text{cm}^2/\text{cm}=\text{cm}$)

σ is the conductivity of the material (expressed in S/cm)

ε is the permittivity of the material (expressed in F/cm)

ε_r is the relative permittivity of the material and is the permittivity of the material/permittivity of the vacuum (8.8×10^{-14} F/cm)

Unfortunately, there is no general agreement on how to express the dielectric properties of the materials and different parameters and symbols will be found the literature. The following list summarizes the most commonly used parameters and their relationships. It must be noticed that the proper characterization of a dielectric material requires two parameters for each frequency.

Table A. 1. Dielectric properties.

Parameter	Symbols	Units	Equations
conductivity	σ, κ	S/cm	$\mathbf{Y} = G + jB = K(\sigma + j\omega\epsilon); \quad \sigma = G/K$
permittivity	ϵ	F/cm	$\mathbf{Y} = G + jB = K(\sigma + j\omega\epsilon); \quad \epsilon = B/(\omega K)$
relative permittivity	ϵ_r	no units	$\epsilon_r = \epsilon/\epsilon_0$
resistivity	ρ	$\Omega \cdot \text{cm}$	$\mathbf{Z} = 1/\mathbf{Y} = (R + jX); \quad R=(1/K) \cdot \rho; \quad \rho \neq 1/\sigma$

Notes:

1. in some studies, specially those working at a single frequency, the conductivity and resistivity values are not strictly treated. In those cases, it is assumed that the imaginary part is not relevant (an assumption that is quite well-founded in BM field) and, consequently, the following equations are adopted: $\mathbf{Y} = |\mathbf{Y}| = K \cdot \sigma$; $\mathbf{Z} = |\mathbf{Z}| = (1/K) \cdot \rho$; $\rho = 1/\sigma$
2. the 'complex conductivity' and 'complex permittivity' parameters have also been defined and are being used by some authors (see [2])

As a didactical example now it will be shown how the conductivity (expressed in Siemens/centimeter, S/cm) and the relative permittivity ($\epsilon_r = \epsilon/\epsilon_0$, no units) can be obtained from the measured impedance values:

Imagine that the impedance values of the previous circuit (R1 in parallel with R2 and C in series (Figure A. 16)) have been obtained by measuring the following piece of material.

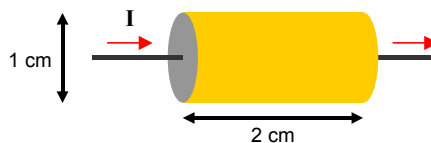


Figure A. 20. Measurement cell example.

Since the admittance ($\mathbf{Y} = G + jB = G + j\omega C = K(\sigma + j\omega\epsilon) = (\text{section}/\text{length})(\sigma + j\omega\epsilon)$) is directly related with the parameters of interest, the first step is to obtain it by inverting the impedance ($\mathbf{Y} = 1/\mathbf{Z}$). Then, the real part (G) and the imaginary part (B) of \mathbf{Y} can be isolated. The following plot shows the conductance (G) and the susceptance (B)

expressed in Siemens(S). Observe that this is not a Bode plot (the Y axis is expressed in linear units).

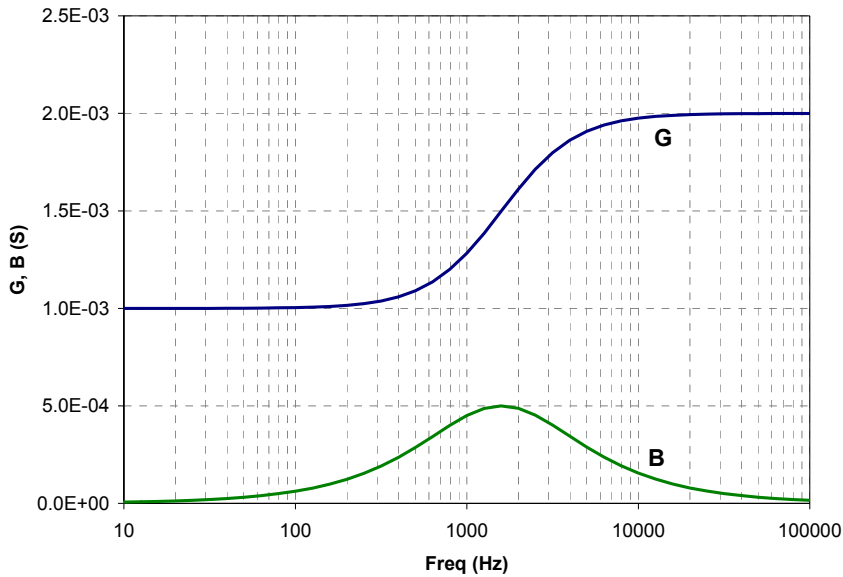


Figure A. 21. Conductance and susceptance plot.

A Wessel diagram can also be plot with the conductance and susceptance values.

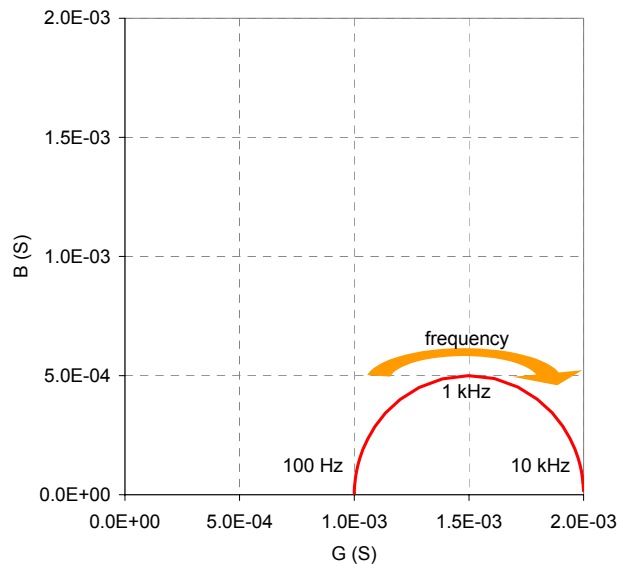


Figure A. 22. Wessel diagram with the conductance and the susceptance values.

The scaling factor (K) is $(\pi \times 1 \text{ cm}^2)/(2 \text{ cm}) = 1.57 \text{ cm}$. Then, the conductivity ($\sigma = G/K$) and the relative permittivity ($\epsilon_r = \epsilon/\epsilon_0$, $\epsilon_0 = 8.8 \times 10^{-14} \text{ F/cm}$; $\epsilon = B/(\omega K) = B/(2\pi fK)$) can be obtained from the conductance (G) and susceptance (B) values:

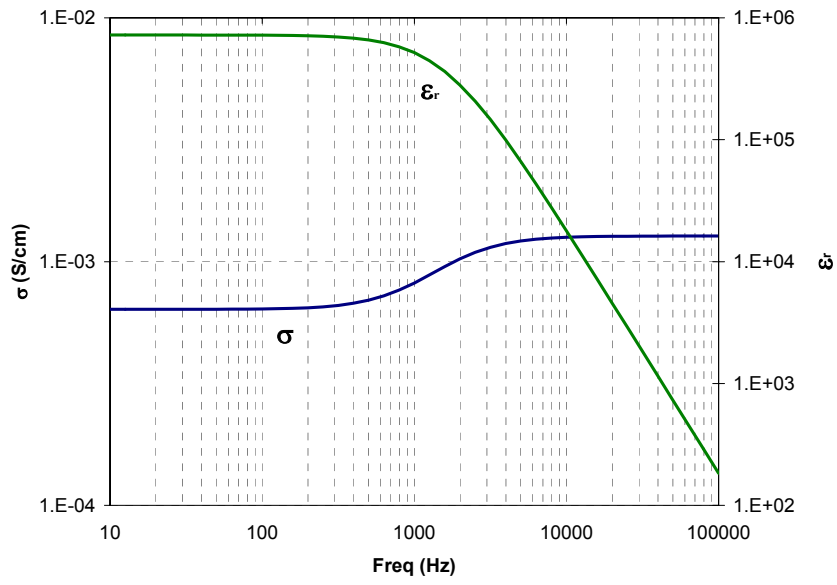


Figure A. 23. Conductivity and relative permittivity plot.

A.3. Electrical bioimpedance

Electrical bioimpedance is defined as the measurement of the electrical impedance of a biological sample. This parameter *per se* is of minor importance. However, it can reflect some interesting physiological conditions and events.

Schwann [41] defined three frequency regions for the dielectric properties of biological materials from the observed main dispersions of the conductivity and the permittivity (see the plot below).

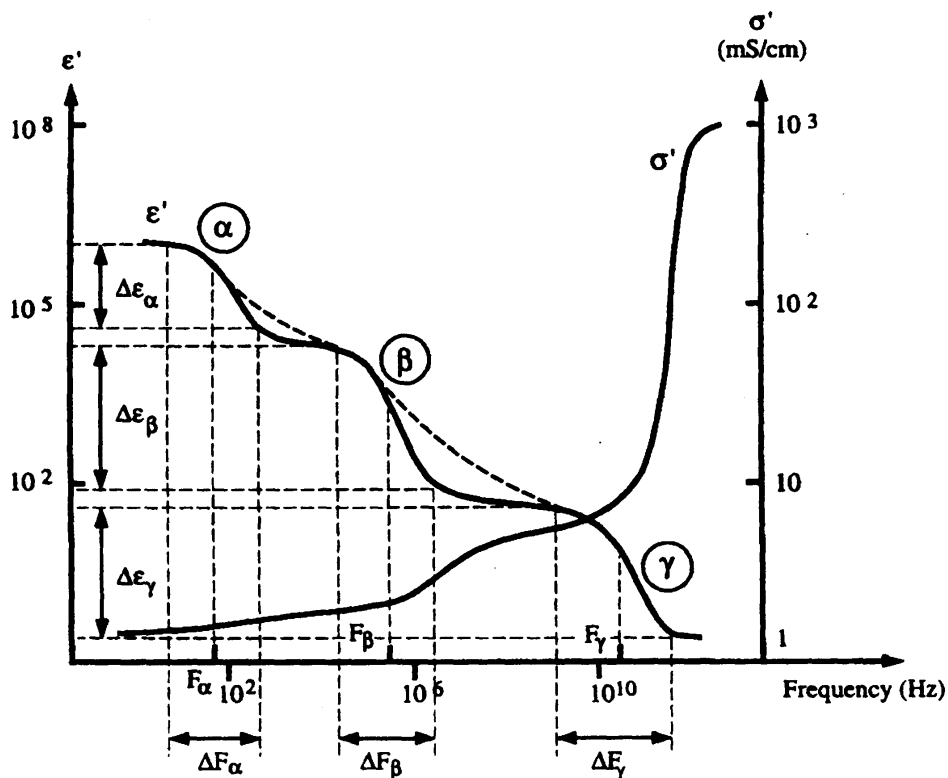


Figure A. 24. Frequency dependence of the conductivity and the permittivity of living tissues (source: [3]).

The large dielectric dispersions appearing between 10 Hz and tens of MHz (α and β dispersion regions) are generally considered to be associated with the diffusion processes of the ionic species (α dispersion) and the dielectric properties of the cell membranes and their interactions with the extra and intra-cellular electrolytes (β dispersion). The dielectric properties at the γ region are mostly attributed by the aqueous content of the biological species and the presence of small molecules [42]. Some authors also reference a fourth main dispersion called δ between the β and γ the dispersions, around 100 MHz, [43] that would be caused by the dipolar moments of big molecules such as proteins.

The reader just needs to keep in mind that the purpose of this paper is to describe the tissue impedance changes observed between 100 Hz and 10MHz and, therefore, we will be dealing with the so called **β dispersion**.

A.3.1. Origin of the β dispersion

The cell is the basic unit of living tissues. Its basic structure (a phospholipid bilayer membrane that separates the intracellular medium from the extracellular medium) determines the tissue electrical impedance from some Hz to several tens of MHz.

Extracellular medium

From the electrical point of view, the extracellular medium can be considered as a liquid electrolyte (ionic solution). By far, the most important ions are Na^+ (~ 140 mM) and Cl^- (~100 mM). Thus, the electrical properties depend on all physical or chemical parameters that determine their concentration or mobility.

The **temperature** plays an important role in ionic conductance. As it has been said, the viscosity of the solvent decreases as the temperature rises, increasing the ion mobility and, consequently, decreasing the resistance. Specifically, there exist a linear relation between temperature and ionic conductance (1/resistance) that lies around 2%/°C. However, this temperature coefficient is not fixed and should be determined for each kind of tissue [44].

For small **ion concentrations** or small concentration changes, a linear relationship between conductance and concentration can be assumed. Of course, other ions than Na^+ and Cl^- or charged molecules (proteins) will contribute to the overall conductivity (see Table A. 2).

In most tissues, the **pH** is in the range 6-8. Hence the concentration of H_3O^+ ions is very low (~ μM) and does not contribute significantly.

Intracellular medium

The ionic concentration of the intracellular medium is similar to the concentration of the extracellular medium (180 meq/L against 153 meq/L). In this case, the important charge carriers are K^+ , protein- and $\text{HPO}_4^{2-} + \text{SO}_4^{2-} +$ organic acids.

Besides the ions and other charged molecules, inside the cell it is possible to find numerous membrane structures with a completely different electrical response. These membranes are formed by dielectric materials and their conductivity is very low. Thus, the impedance of the intracellular medium must be a mixture of conductive and

capacitive properties. However, for simplification, it is generally accepted that the intracellular medium behaves as a pure ionic conductor.

Table A. 2. Concentration of electrolytes in body liquids (source: [2]).

	cations (meq/L)		anions (meq/L)		
	extracellular	intracellular	extracellular	intracellular	
Na ⁺	142	10	Cl ⁻	103	4
K ⁺	4	140	HCO ₃ ⁻	24	10
Ca ²⁺	5	10 ⁻⁴	protein-	16	36
Mg ²⁺	2	30	HPO ₄ ²⁻ + SO ₄ ²⁻	10	130
H ⁺	4×10 ⁻⁵	4×10 ⁻⁵	+ organic acids		
Sum	153	180	Sum	153	180

Cell membrane

The cell membrane has a passive role (to separate the extra and the intracellular media) and an active role (to control the exchange of different chemical species).

The passive part of the cell membrane is the bilayer lipid membrane (BLM). This film (~7nm thick) allows lipids and water molecules to pass through it but, in principle, it is completely closed for ions. Its intrinsic electrical conductance is very low and it can be considered a dielectric. Therefore, the structure formed by the extracellular medium, the BLM and the intracellular medium is a conductor-dielectric-conductor structure and it behaves as a capacitance (~1 μF/cm²).

In parallel with the BLM there are embedded proteins, transport organelles, ionic channels and ionic pumps. These structures are the basic elements of the membrane active role. Of particular interest to us are the ionic channels and the ionic pumps.

The **ionic channels** are porous structures that allow some ions to flow from the outside to inside of the cell or vice versa or to flow from one cell to another one (**gap junctions**). These structures are selective to ions and can be opened or closed by some electrical or chemical signals.

The **ion pumps** are energy-consuming structures that force some ions to flow through the membrane. Apart from creating a DC voltage difference across the membrane, they are responsible of maintaining the hydrostatic cellular pressure and their failure yields to cellular edema.

A.3.2. Equivalent circuits and models

It is desirable to depict equivalent circuit models of the tissue bioimpedance because they are useful to attribute a physical meaning to the impedance parameters. Now, from what has been said about the main constituents of the cell, a simple electrical model for the cell can be induced (Figure A. 25). The current injected into the extracellular medium can flow through the cell across the BLM (C_m) or across the ionic channels (R_m) or can circulate around the cell (R_e). Once the current is into the cell it 'travels' through the intracellular medium (R_i) and leaves the cell across the membrane ($R_m \parallel C_m$)

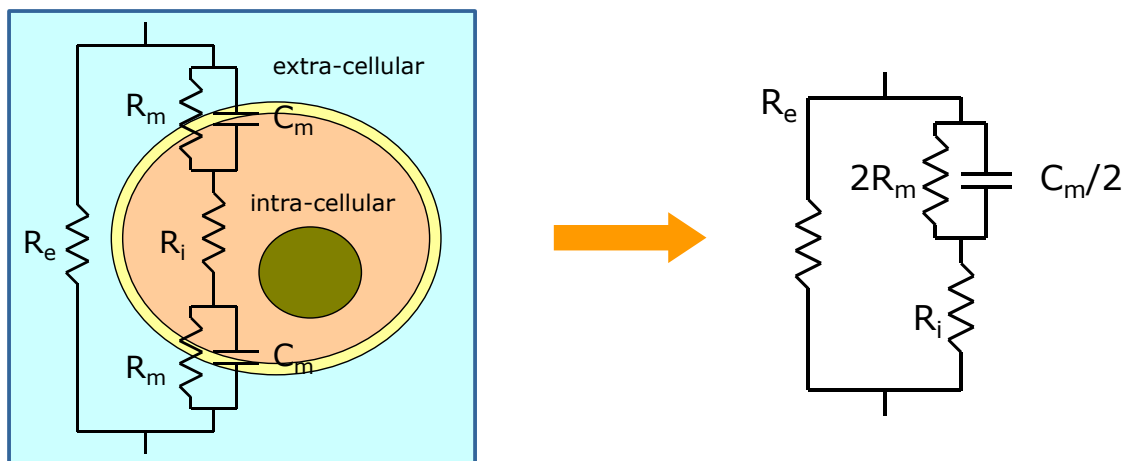


Figure A. 25. Simple circuit model of a single cell.

The circuit on the right is equivalent to the left model after performing some simplifications (resistances in series and capacitances in parallel). The same simplifications can be applied to reduce a tissue composed by many cells to a single cell equivalent circuit.

Usually, the membrane conductance is very low and R_m is ignored. In this case, the equivalent circuit is very simple and a single dispersion exists (see the last circuit example, Figure A. 16). This model has been adopted by many authors and is used to explain the impedance measurements from DC to some tens of MHz. At low frequencies (<1 kHz) most of the current flows around the cell without being able to penetrate into the cell. At high frequencies (> 1 MHz) the membrane capacitance is no impediment to the current and it flows indiscriminately through the extra and intracellular media.

The previous model works reasonably well for dilute cell suspensions. However, the tissue bioimpedance tends to be more complex than that and it is not unusual to observe two superimposed dispersions in the frequency band from 10 Hz to some MHz⁸. An example is the myocardial muscle [45]. This fact means that another

⁸ In this situation, two arcs will be observed on the Wessel diagram.

resistance-capacitance couple should be added to mimic the bioimpedance results. In the case of the myocardium, this second dispersion is attributed to the significant presence of gap junctions [31].

Furthermore, it is necessary to substitute the capacitance in the previous dispersion models by a part called **Constant Phase Element (CPE)** in order to fit accurately the modeled impedance values to the actual bioimpedance measurements. The CPE is not physically realizable with ordinary lumped electric components but it is usually described as a capacitance that is frequency dependent. The impedance of the CPE is:

$$Z_{\text{CPE}} = \frac{1}{(j \cdot 2\pi \cdot f \cdot C)^\alpha}$$

The α parameter usually is between 0.5 and 1. When it is 1 the behavior of the CPE is exactly the same of an ideal capacitance.

The physical meaning of the CPE is not clearly understood. Some authors suggest that α can be regarded as a measure of a distribution of resistance-capacitance combinations. That is, the tissue is not homogeneous and the sizes of the cells are randomly distributed, thus, the combination of the equivalent circuits can differ from the simple RC model.

When the CPE is included in the simple bioimpedance equivalent circuit (a resistance-capacitance series combination in parallel with a resistance), the expression of the impedance is:

$$Z = R_\infty + \frac{\Delta R}{1 + (j \cdot 2\pi \cdot f \cdot \tau)^\alpha}$$

This expression, called **Cole equation**, was found by Cole in 1941 and is used by most authors in the bioimpedance field to describe their experimental results. Hence the tissue bioimpedance is characterized with four parameters: R_∞ , ΔR , α and τ . The parameter R_∞ represents the impedance at infinite frequency (only resistive part), $R_0 (= R_\infty + \Delta R)$ is the impedance at frequency 0 Hz, τ is the time constant ($\Delta R \cdot C$) and α is the α parameter of the CPE.

The resistive values (R_∞ , ΔR , R_0) are usually scaled to resistivity values by using the by the cell constant. The α and τ are not dependent on the cell dimensions and, therefore, do not need to be scaled.

In the representation of the Cole equation on the Wessel diagram, the arc is no longer a semicircle centered in the real axis. Instead of that, the semicircle center is above the real axis and the arc is apparently flattened. That displacement depends on the value of α ($\alpha = 1 \Rightarrow$ semicircle centered on the real axis).

The following Wessel diagram shows an actual bioimpedance multi-frequency measurement (**bioimpedance spectrometry**) from a rat kidney. Observe that the Cole model fits the actual data and that it is equivalent to a semicircle centered below the real axis (take into account that the imaginary axis has been inverted)

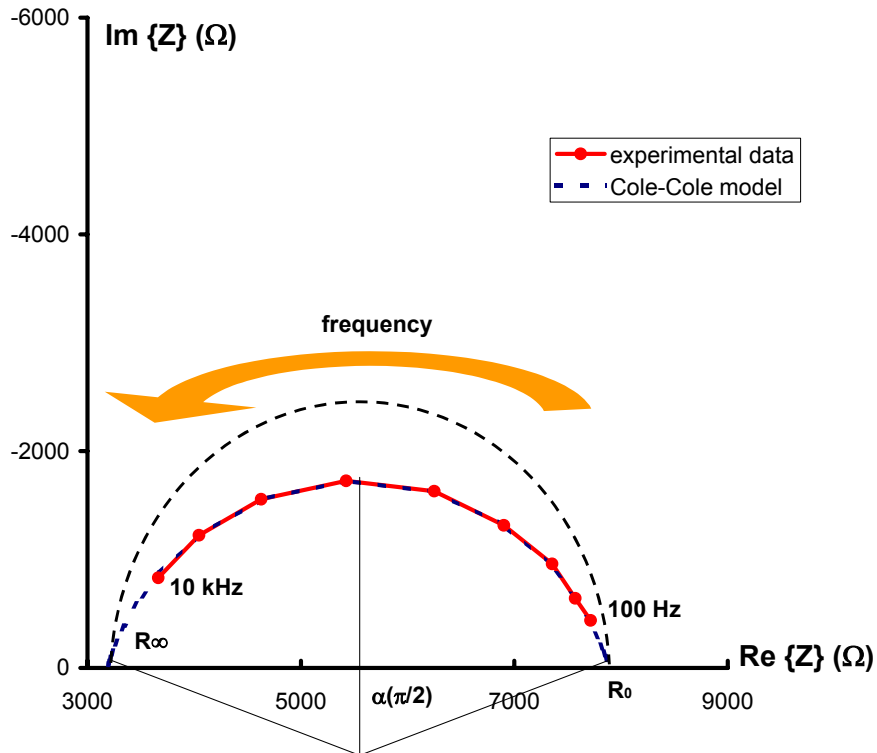


Figure A. 26. Wessel diagram of an actual bioimpedance measurement and the superimposed Cole model results.

In the case that two or more dispersions are observed (e.g. in the myocardium), the above equation is expanded to include the model of each dispersion.

$$Z = R_{\infty} + \frac{\Delta R_1}{1 + (j \cdot 2\pi \cdot f \cdot \tau_1)^{\alpha_1}} + \frac{\Delta R_2}{1 + (j \cdot 2\pi \cdot f \cdot \tau_2)^{\alpha_2}} + \dots$$

Hence the characterization parameters are: R_{∞} , ΔR_1 , α_1 , τ_1 , ΔR_2 , α_2 , τ_2 ...

It must be said that some authors renounce to depict equivalent circuits of the bioimpedance because they consider them a dangerous practice that can produce erroneous interpretations [46]. The same impedance measurements can be interpreted as completely different circuits with different topologies and values. Thus, these authors chose a mathematical model (Cole-Cole equation) to describe their results without trying to interpret them.

A.4. Bioimpedance monitoring

The electrical impedance of a living tissue can be continuously measured in order to determine its patho-physiological evolution. Some pathologies like ischemia, infarct or necrosis imply cellular alterations that are reflected as impedance changes. As it was described in the introduction, the bioimpedance monitoring has been proposed for myocardium ischemia detection, for graft viability assessment and for graft rejection monitoring. In most of the cases, the event is detected or monitored because an alteration of the extra-intracellular volumes occurs.

The following figure illustrates how ischemia is monitored by bioimpedance measurements. During the normoxic condition, a significant amount of low frequency current is able to flow through the extracellular spaces. When ischemia and the following lack of oxygen (hypoxia) is caused by any means, the cells are not able to generate enough energy to feed the ion pumps and extracellular water penetrates into the cell. As a consequence, the cells grow and invade the extracellular space [47]. This causes a reduction of the low frequency current that yields an impedance modulus increase at this low frequency. Thus, the bioimpedance measurement at low frequencies is an indicator of the tissue ischemia.

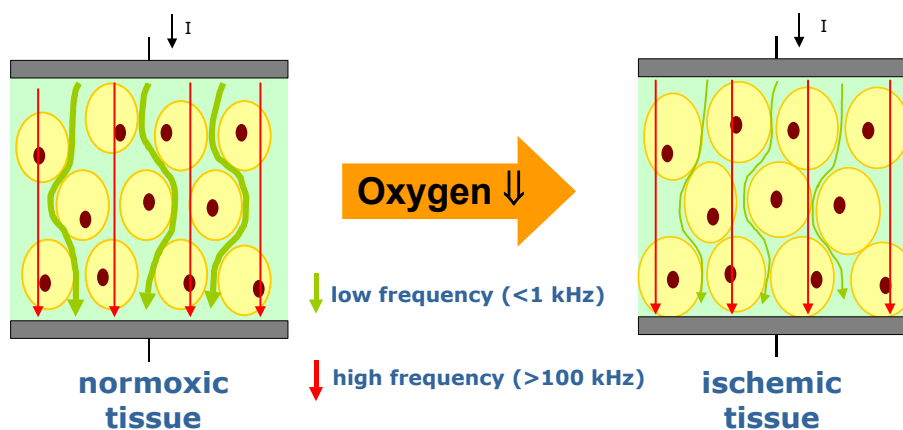


Figure A. 27. Schematic representation of the impedance modulus increase at low frequencies due to the cell swelling caused by ischemia.

This simplistic description of the ischemia-impedance relationship could be not correct for cells containing gap junctions. In those cases (e.g. myocardium) the observed impedance increase at low frequencies is mostly attributed to the closure of the gap junctions [31;48].

As an example, the following graph shows the evolution of the impedance modulus at 1 kHz for six impedance probes inserted in a beating pig heart subjected to regional ischemia (see the method in [48]). Three of them are within a normoxic area and the other three are within the area influenced by the ischemia.

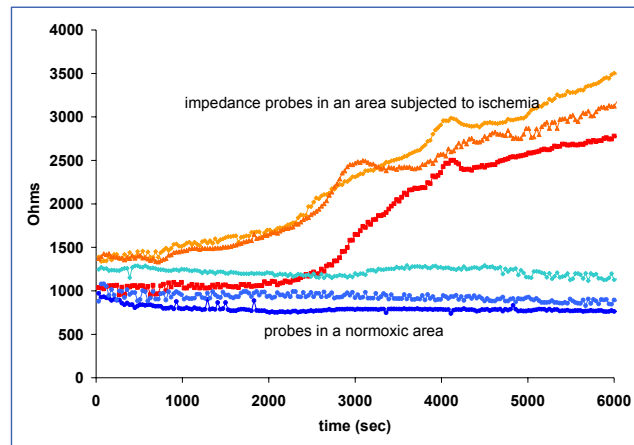


Figure A. 28. Impedance modulus measurements (1kHz) of a pig myocardium subjected to regional ischemia.

The necrosis process that follows a long ischemia period can also be detected because the loss of membrane integrity allows continuity between the extra and intra-cellular media and, consequently, the impedance magnitude at low frequencies decreases [29].

Single-frequency measurements are relatively easy performed and provide the necessary information to follow the ischemia processes. Therefore, some researchers have promoted them as the basis for a clinical parameter to monitor the tissue condition. However, multiple-frequency bioimpedance measurements (**bioimpedance spectrometry**) and the subsequent characterization (Cole model) provide additional information and improve the reproducibility of the results [30].

The following graphs show the results from the Cole impedance characterization of a series of rat kidneys during cold preservation (see [49] or [50] for details). Two groups where studied:

- CI group: kidneys preserved following a standard transplantation process (perfusion of University of Wisconsin solution + cold storage at 4 °C).
- WI group: kidneys preserved in the same manner as the CI group but subjected to a previous warm ischemia of 45 minutes before extraction.

Observe that R_0 , R_∞ and τ tend to converge for both groups after 24 hours of preservation while α diverges. This fact indicates that α is related with some kind of tissue damage different from cell edema and is an example of the usefulness of the bioimpedance spectrometry compared to single-frequency bioimpedance measurements.

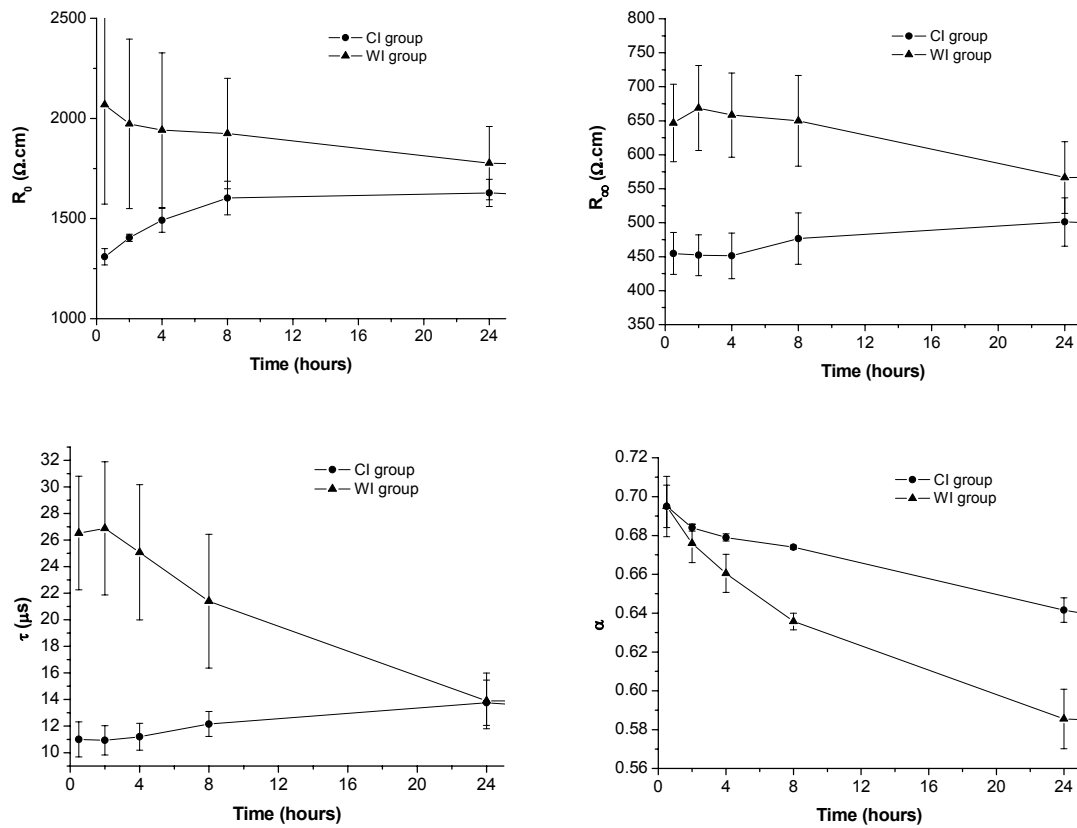


Figure A. 29. Cole-Cole characterization of multi-frequency bioimpedance measurements (see the text).

A.4.1. Computer Simulations

In order to clarify the relationships between cell and tissue structures and the bioimpedance measurements at the β dispersion region, here are shown the results of some computer simulations performed with a custom developed software package⁹

The simulator allows to draw a rough two-dimensional map of the tissue or cell structure. Then, each pixel (each square of the map grid) is converted into its equivalent circuit elements (resistors and capacitors) and the impedance value is computed with the aid of a circuit analysis tool (SPICE).

⁹ This simulator and the details concerning its implementation, features and limitations are available at (<http://www.cnm.es/~mtrans/BioZsim/>). Other similar simulations are shown in chapter 4.

Cellular edema

One of the most accepted explanations to the fact that impedance modulus at low frequencies increases during ischemia is the fact that the cell edema, induced by the lack of oxygen, limits the extracellular space and that causes an increase of R_0 .

The following sequence of tissue simulations tries to mimic this effect. From map 0 to map 2, cells size increases progressively with the consequent reduction of extra-cellular space. The "impedance measurement" is performed with two electrodes placed on both sides of the sample.

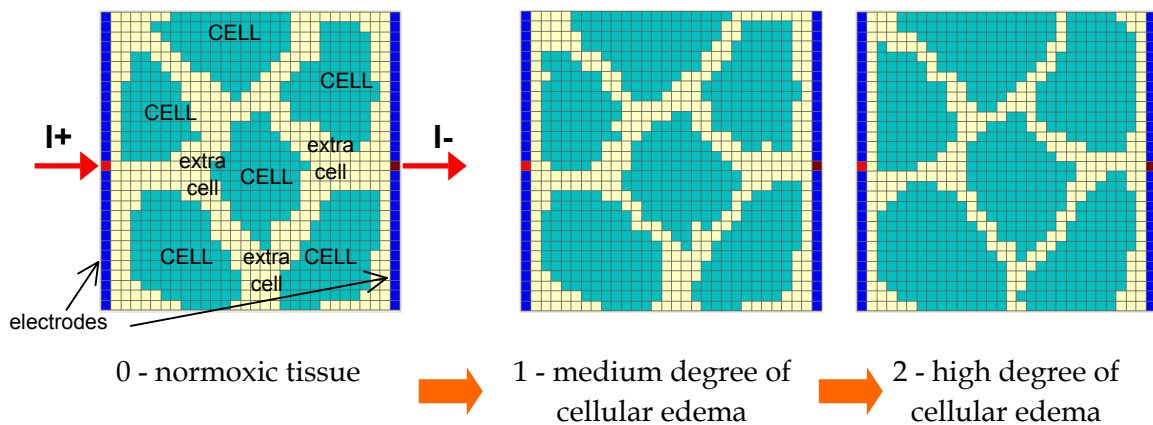


Figure A. 30. Sequence of tissue simulations mimicking the cellular edema caused by ischemia.

Table A. 3. Constants of interest taken into account by the simulator.

simulated slab thickness	50 μm
pixel size	5 $\mu\text{m} \times 5 \mu\text{m}$
number of pixels	30 \times 30
electrode resistivity	0 $\Omega\cdot\text{cm}$
intracellular resistivity	100 $\Omega\cdot\text{cm}$
extracellular resistivity	100 $\Omega\cdot\text{cm}$
membrane capacitance	1 $\mu\text{F}/\text{cm}^2$
membrane resistance	1 $\text{G}\Omega\cdot\text{cm}^2$ (infinite)

The results given by the simulator are:

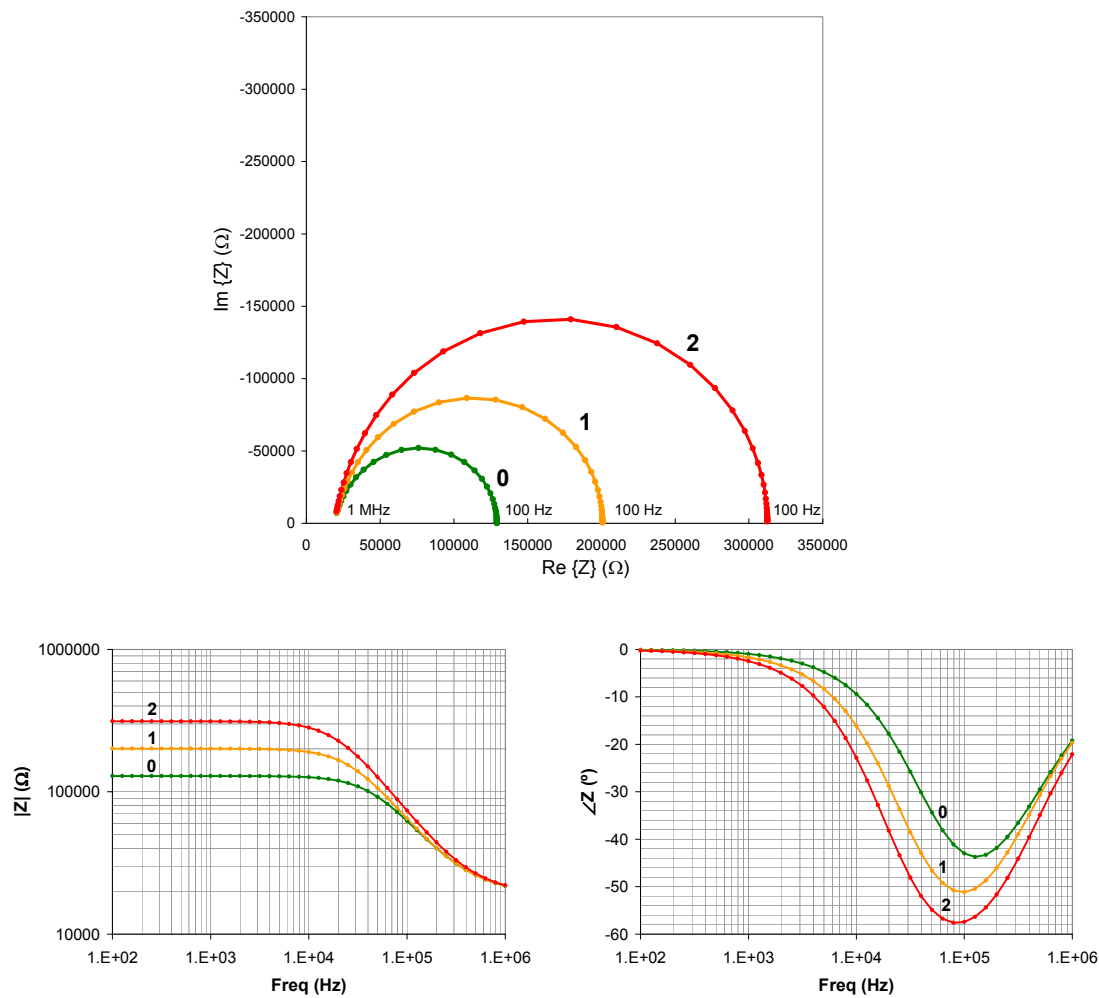


Figure A. 31. Results from the simulation.

From the Wessel or Bode plots it can be seen that the impedance modulus at low frequencies indeed increases significantly following the cell edema process. At high frequencies this sensitivity is poorer, even negligible, since the current flows freely through the tissue without being disturbed by the dielectric cell membranes.

In this hypothetical case, three frequencies could be considered to develop a single-frequency ischemia detector:

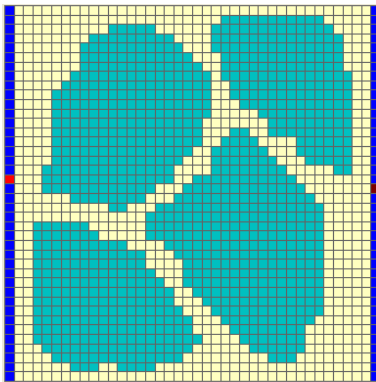
1. <10 kHz: the impedance modulus is very sensitive to cell edema.
2. ~ 10 kHz: both, the impedance modulus and phase are sensitive to cell edema.
3. ~ 100kHz: at these frequencies around the central frequency of the single dispersion the impedance phase is quite sensitive to cell edema.

In general, the impedance modulus is easier to measure than the phase, however, the phase has the advantage of being cell constant independent.

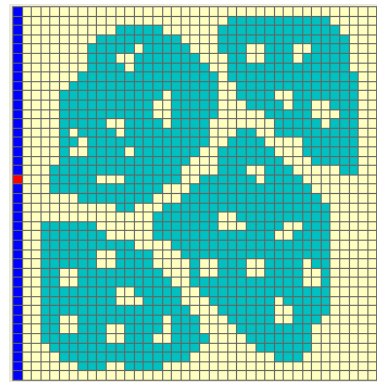
Cellular organelles

The presence of organelles inside the cells is sometimes mentioned as the possible cause of secondary impedance dispersions observed at higher frequencies than the main β dispersion. This hypothesis is based on the fact that organelles can be considered as cells inside the cell (i.e. an electrolytic medium contained in a dielectric membrane immersed into an electrolytic medium). Since they are smaller than the cells and the rest of parameters are more or less equal (ionic conductances and membrane capacitance) their relaxation frequency is higher than the relaxation frequency associated to the cells.

The following simulations try to show the effect on the impedance measurements of this 'cells' contained into the cells. Two tissues are simulated: 1) tissue made up of cells without organelles and 2) tissue made up of cells containing organelles.



1- cells without organelles



2- cells with organelles

Figure A. 32. Simulated tissue structures.

Table A. 4. Constants of interest taken into account by the simulator.

simulated slab thickness	50 μm
pixel size	5 $\mu\text{m} \times 5 \mu\text{m}$
number of pixels	40 \times 40
electrode resistivity	0 $\Omega\cdot\text{cm}$
intracellular resistivity	100 $\Omega\cdot\text{cm}$
extracellular resistivity	100 $\Omega\cdot\text{cm}$
membrane capacitance	1 $\mu\text{F}/\text{cm}^2$
membrane resistance	1 $\text{G}\Omega\cdot\text{cm}^2$ (infinite)

The results given by the simulator are:

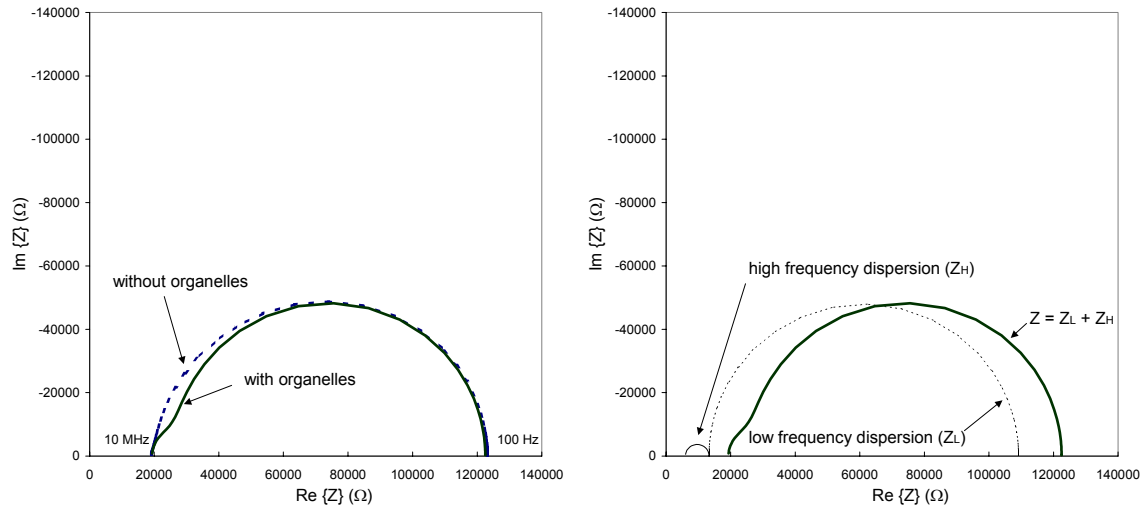


Figure A. 33. Simulated Wessel diagrams of both tissue structures. The diagram on the right shows the two dispersions that can be combined to create the simulated dispersion of the case corresponding to the cells with organelles.

The presence of organelles distorts the semicircle in the Wessel diagram. Such a distortion can be modeled as second high frequency dispersion as it is shown on the right. Hence the bioimpedance measurement is the sum of a low frequency dispersion (Z_L) and a secondary high frequency dispersion (Z_H).

Observe that in the Bode plots it becomes clear that the effect of the secondary dispersion is manifested at high frequencies (1 MHz).

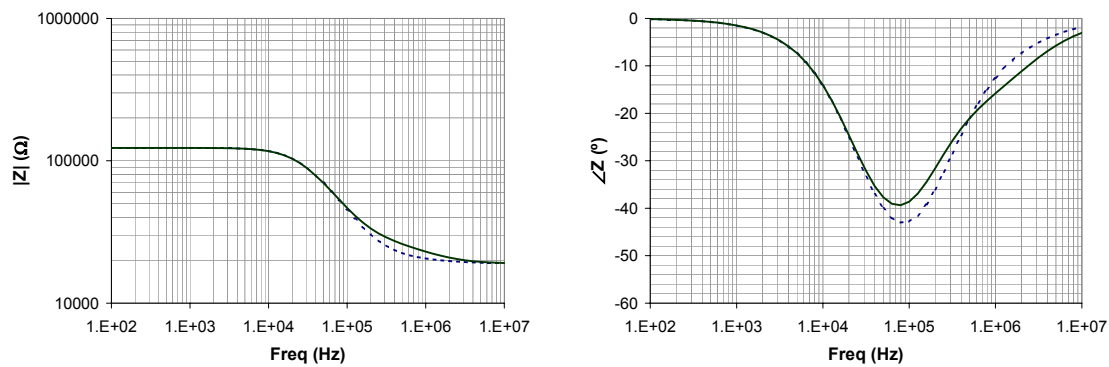


Figure A. 34. Simulated Bode plots of both tissue structures.

Gap junctions

In some tissues, such as the myocardium, cells are electrically connected through gap junction channels. Gap junction channels are physical structures formed by large proteins on the BLM that connect the intracellular media of adjacent cells. They are permeable for various ions and for small molecules with a molecular weight of up to 1000 D. Their primary role is the communication between cells and for that purpose their conductance can be controlled by the cells.

Some researchers [31;48] postulate that gap junction channels play an important role in the observed impedance modulus increase observed during ischemia in tissues such as the myocardium and the liver. The modulus increase is explained as the consequence of the progressive closure of the gap junction channels. It is also affirmed that gap junctions are responsible for the existence of a low frequency dispersion.

In the following simulations the effect of the gap junctions closure in a tissue is modeled: 0) opened gap junctions channels (gap junction resistance = $1 \Omega \cdot \text{cm}^2$). and 1) closed gap junctions channels (gap junction resistance = $100 \Omega \cdot \text{cm}^2$).

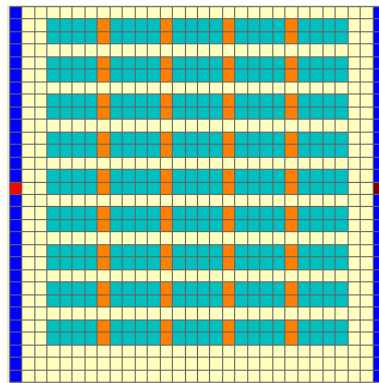


Figure A. 35. Simulated tissue structure containing gap junctions.

The above map is used for both simulations. Observe that gap junctions (orange squares) are only located on the extremes of the cells.

Table A. 5. Constants of interest taken into account by the simulator.

simulated slab thickness	20 μm
pixel size	25 $\mu\text{m} \times 25 \mu\text{m}$
number of pixels	30 \times 30
electrode resistivity	0 $\Omega \cdot \text{cm}$
intracellular resistivity	100 $\Omega \cdot \text{cm}$
extracellular resistivity	100 $\Omega \cdot \text{cm}$
membrane capacitance	1 $\mu\text{F} / \text{cm}^2$
membrane resistance	1 $\text{G}\Omega \cdot \text{cm}^2$ (infinite)
gap junctions resistance	1 $\Omega \cdot \text{cm}^2 \Rightarrow 100 \Omega \cdot \text{cm}^2$
gap junction separation	1 μm

The results are:

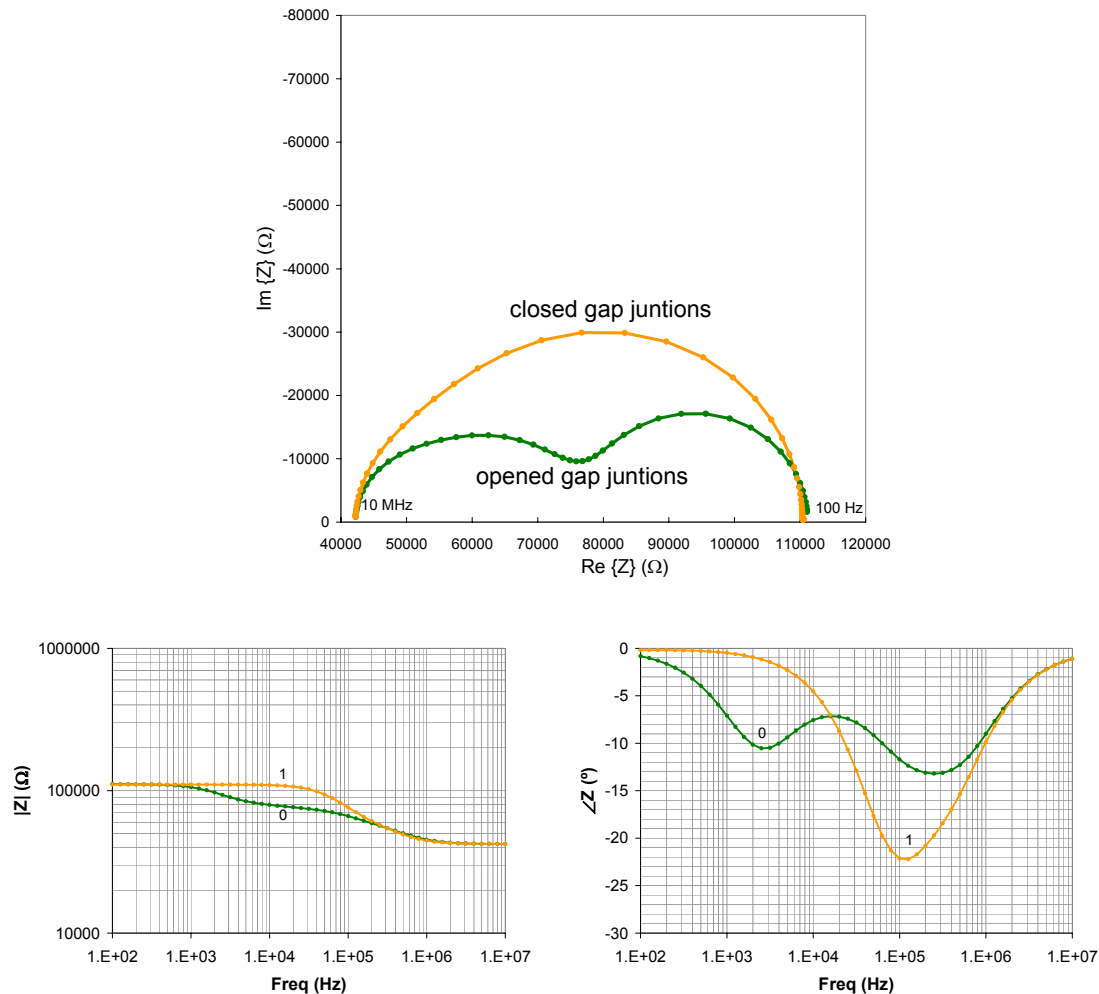


Figure A. 36. Simulated Wessel diagram and Bode Plots of a tissue containing gap junctions.

The gap junctions conductance indeed justifies the presence of two distinguishable dispersions. The high frequency dispersion is associated to the cell size (observe that when the gap junctions are closed the dispersion is located approximately at the same frequency). The low frequency dispersion is associated to the macro-cell structure made up of five cells connected through the gap junction channels. In the extreme case that the resistance of the gap junctions is 0Ω , a single dispersion at low frequencies would be observed and that would correspond to a tissue composed of very long cells ($850 \mu\text{m} \times 50 \mu\text{m} \times 20 \mu\text{m}$).

The impedance modulus at medium frequencies ($\sim 10 \text{ kHz}$) increases following the gap junctions closure. However, the impedance modulus at very low frequencies is not influenced by the gap junctions closure because the current is completely confined to the extra-cellular medium. Hence the affirmation that impedance modulus increase according to gap junctions closure is only valid beyond a certain frequency.

A.4.2. Measurement methods and practical constraints

Although it is not the objective of this paper to describe the instrumentation used for bioimpedance monitoring, some issues concerning the measurement method need to be presented.

Electrode-electrolyte interface impedance

In order to avoid tissue damage or electrode degradation, most electrodes used for bioimpedance measurements are made with noble metals (Pt or Au) or stainless steel. In the interface of these electrodes with the tissue, no electronic exchange reaction (redox) exists, and, as a consequence, the direct current is not able to flow through them from the metal to the tissue or vice versa. Because of that, these electrodes are called blocking electrodes and only the alternating current is able to flow through them¹⁰. Its impedance (electrode-tissue impedance or electrode-electrolyte impedance) is quite similar to a capacitance¹¹ that depends on the electrode area (area \uparrow \Rightarrow electrode impedance \downarrow) and on many uncontrollable factors (temperature, tissue ionic contents, protein adhesion...).

This interface impedance disturbs the bioimpedance measurements, particularly at low frequencies, and must be kept as low as possible. Hence, it is quite common to make use of special fabrication techniques to enlarge the effective area such as electrode surface abrasion or special electrochemical depositions¹².

Four-electrode method

It could be supposed that tissue impedance can be measured by a couple of electrodes attached to the surface of the sample under study. Both electrodes would be used to inject the current and to measure the voltage drop. However, the electrode-electrolyte interface impedances are in series with the sample impedance and, therefore, the measured impedance is the sum of the three impedances ($Z_x + Z_{e1} + Z_{e2}$). Unfortunately, these parasitic impedances are sufficiently large to disturb the measurements, especially at low frequencies. Because of that, an alternative measuring method is used: the current is injected with a couple of electrodes and the resulting voltage drop is measured with another couple of electrodes. This method, known as four-electrode method or tetrapolar method, has been used for more than a century [52] and it ideally cancels the influence of the electrode-electrolyte interface impedance.

¹⁰ That is only true if the applied potential is very low (<1 V), otherwise, electrode exchange reactions occur and DC current flows through the tissue. However, this is an undesired effect because such reactions would damage the tissue and the electrodes.

¹¹ It is commonly modeled as a Constant Phase Element (CPE).

¹² The electrochemical deposit of 'black platinum' on platinum electrodes is one of the of most common techniques [51].

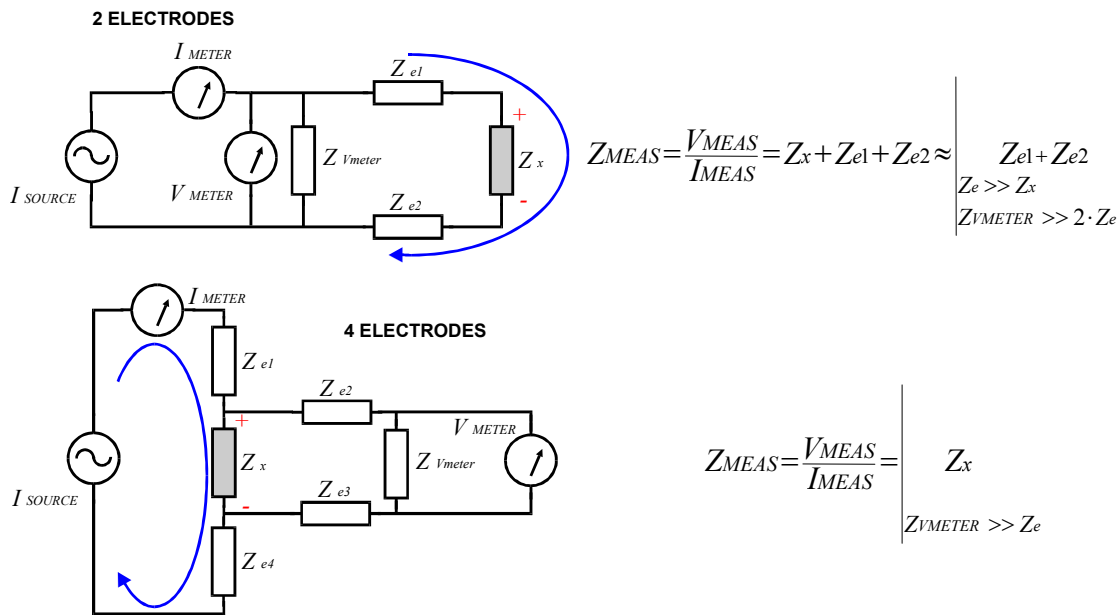


Figure A. 37. Schematic representation of the bipolar and the tetrapolar impedance measurement methods.

Of course, the four-electrode method is not totally free from errors. Other parasitic impedances (e.g. capacitances between wires or instrumentation input impedances) combined with the electrode-electrolyte impedances cause errors at high and low frequencies [53] and that constrains the useful measurement band of the four-electrode method from some Hz to hundreds of MHz.

Under certain circumstances, the measurements performed with two electrodes¹³ can be also acceptable because the electrode impedance is negligible compared to the impedance under test. In those cases, large electrode areas (> 1cm²) and frequencies above 10 kHz are usually employed.

Measurement cell geometry

As it has been explained, the scaling factor that converts the measured values into resistivity or conductivity values (**cell constant**) depends on the geometry and on the configuration of the electrodes used to perform the measurement. In some cases it can be calculated from the geometrical dimensions but in most cases it is more practical to extract its value from the measurement of a sample with a known resistivity. For instance, a NaCl 0.9% saline solution at 25 °C has a resistivity of 72.8 Ω.cm (conductivity = 13.7 mS/cm) and it is purely resistive (null imaginary part, phase angle = 0°) up to some MHz.

¹³ Three electrode configurations have also been used [54]. They are also influenced by the electrode impedance but to a less degree than two electrode configurations.

Another important issue related with the geometrical design of the electrodes is the **spatial resolution** [55]. That is, the tissue volume around the electrodes that will contribute to the measured impedance. In some cases it will be desired to detect localized events and a high spatial resolution will be necessary. In other cases it will be desired to avoid the tissue heterogeneity and a low resolution configuration will be required.

Impedance probes

Standard ECG electrodes or novel metal plates can be applied on the tissue surface under study to monitor the bioimpedance. However, this approach presents some important drawbacks:

- modifications of the tissue surface (e.g. caused by movements) will change impedance cell geometry and, consequently, the impedance measurements will be altered (measurement artifacts).
- the effective measurement volume is too much superficial.
- the presence of a thin film of blood or plasma will hamper the impedance measurement [56].

Some successful tissue bioimpedance measurements have been carried out with such kind of electrode set ups but in those cases the fixation method became crucial and, usually, resulted in high invasive devices.

For those reasons, the impedance probe used in most *in vivo* studies consists in an array of four equidistant needle shaped electrodes (four-electrode plunge probe). The current is injected into the sample through the two external electrodes and the voltage drop is measured with the inner electrodes [55].

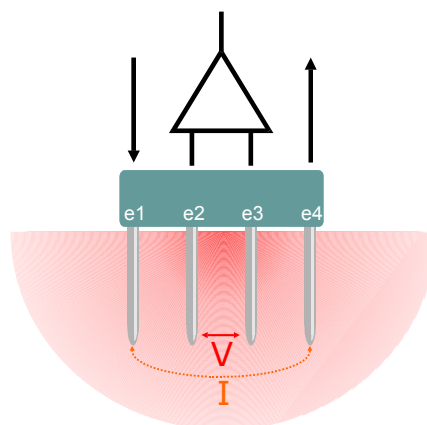


Figure A. 38. Four-electrode plunge probe.

Recently, another approach has been proposed: to use needle shaped probes with four planar electrodes on its shaft [57]. This configuration has some advantages: it is

minimally invasive, it enables inner tissue measurements and it is appropriate for planar fabrication techniques (microelectronics). The use of microelectronic fabrication techniques implies that other devices can be integrated on the same needle to increase the system performance.

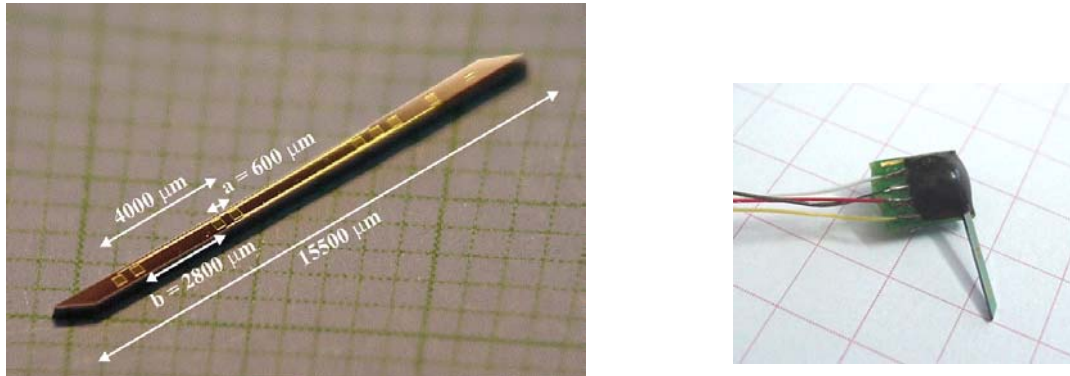


Figure A. 39. Needle shaped silicon probes.

A.5. Recommended literature

Grimnes S., Martinsen O.G., 'Bioimpedance & Bioelectricity Basics', Academic Press, ISBN-0-12-303260, <http://www.fys.uio.no/publ/bbb>, 2000.

Bourne J.R. (ed.), Morucci J.-P., Valentinuzzi M.E., Rigaud B., Felice C.J., Chauveau N., Marsili P.M., 'Bioelectrical Impedance Techniques in Medicine', Critical Reviews in Biomedical Engineering, Vol. 24, Issues 4-6, 1996.

Defelice, L.J., 'Electrical properties of cells: patch clamp for biologists', Plenum Press, New York, 1997.

Horowitz P., Hill W., 'The Art of Electronics', Cambridge University Press; ISBN: 0521370957; 2nd edition (1989).

A.6. Recommended downloadable documents and web sites

Casas O., 'Contribución a la obtención de imágenes paramétricas en tomografía de impedancia eléctrica para la caracterización de tejidos biológicos', Ph.D. Thesis, Universitat Politècnica de Catalunya, Barcelona, 1998. (Spanish)
<http://petrus.upc.es/~wwwdib/tesis/Oscar/resumen.html>

Scharfetter H. Structural modeling for impedance-based non-invasive diagnostic methods. Habilitation thesis, University of Technology Graz, 2000. (English)
<http://www.cis.tugraz.at/bmt/scharfetter/Bioimpedance.htm>

Songer, J.E. 'Tissue Ischemia Monitoring Using Impedance Spectroscopy: Clinical Evaluation' MS Thesis, Worcester Polytechnic University, 2001, (English)
<http://www.wpi.edu/Pubs/ETD/Available/etd-0827101-212826/>

International committee for the promotion of research in bioimpedance (ICPRBI)
<http://www.isebi.org/>

Concise information about T-scan (breast imaging):
<http://imagnis.com/t-scan/index.asp#main>

Electrical Impedance Tomography group:
<http://www.eit.org.uk/index.html>

References

1. McAdams, E. T. and Jossinet, J., "Tissue impedance: a historical overview," *Physiol Meas.*, vol. 16, no. 3, pp. 1-13, 1995.
2. Grimnes, S. and Martinsen, Ø. G., *Bioimpedance and bioelectricity basics* London: Academic Press, 2000.
3. Morucci, J.-P., Valentinuzzi, M. E., Rigaud, B., Felice, C. J., Chauveau, N., and Marsili, P.-M., "Bioelectrical Impedance Techniques in Medicine," *Critical Reviews in Biomedical Engineering*, vol. 24, no. 4-6, pp. 223-681, 1996.
4. Scharfetter, H., "Structural modeling for impedance-based non-invasive diagnostic methods." PhD Thesis PhD Thesis, Technical University Graz, 1999.
5. Felice, C. J., Valentinuzzi, M. E., Vercellone, M. I., and Madrid R E, "Impedance bacteriometry: medium and interface contributions during bacterial growth," *IEEE Transactions on Biomedical Engineering*, vol. 39, no. 12, pp. 1310-1313, 1992.
6. Bragos, R., Gamez, X., Cairo, J., Riu, P. J., and Godia, F., "Biomass monitoring using impedance spectroscopy," *Annals of the New York Academy of Sciences*, vol. 873 pp. 299-305, 1999.
7. Keese, C. R. and Giaever, I., "A Biosensor that Monitors Cell Morphology with Electrical Fields," *IEEE Engineering in Medicine and Biology Magazine*, vol. 13, no. 3, pp. 402-408, 1994.
8. Borkholder, D A, "Cell Based Biosensors Using Microelectrodes." PhD Thesis PhD Thesis, Stanford University, 1998.
9. Geddes, L. A. and Baker, L. E., "Detection of Physiological Events by Impedance," in Geddes, L. A. and Baker, L. E. (eds.) *Principles of applied biomedical instrumentation* Third Edition ed. New York: Wiley-Interscience, 1989, pp. 537-651.
10. Walker, D. C., Brown, B. H., Hose, D. R., and Smallwood, R. H., "Modelling the electrical impedivity of normal and premalignant cervical tissue," *Electronics Letters*, vol. 36, no. 19, pp. 1603-1604, 2000.
11. Jossinet, J. and Schmitt, M., "A review of parameters for the bioelectrical characterization of breast tissue," *Annals of the New York Academy of Sciences*, vol. 873 pp. 30-41, 1999.
12. Haemmerich, D., Staelin, S. T., Tsai, J.-Z., Tungjitkusolmun, S., Mahvi, D. M., and Webster, J. G., "In vivo electrical conductivity of hepatic tumours," *Physiol Meas.*, vol. 24 pp. 251-260, 2003.
13. Malich, A., Böhm, T., Facius, M., Kleinteich, I., Fleck, M., Sauner, D., Anderson, R., and Kaiser, W. A., "Electrical impedance scanning as a new imaging modality in breast cancer detection-a short review of clinical value on breast application, limitations and perspectives," *Nuclear Instruments and Methods in Physics Research A*, vol. 497 pp. 75-81, 2003.
14. Benvenuto, A., Beccai, L., Valvo, F., Mencias, A., Dario, P., Carrozza, M. C., Aguiló, J., Ivorra, A., Villa, R., Millán, J., Godignon, P., Bausells, J., and Errachid, A. Impedance microprobes for myocardial ischemia monitoring. 234-238. 12-10-2000. Lyon, France. 1st Annual International IEEE-EMBS Special Topic Conference on Microtechnologies in Medicine and Biology. 12-10-2000.
Ref Type: Conference Proceeding

15. Schwartzman, D., Chang, I., Michele, J. J., Mirotznik, M. S., and Foster, K. R., "Electrical impedance properties of normal and chronically infarcted left ventricular myocardium," *Journal of Interventional Cardiac Electrophysiology*, vol. 3 pp. 213-224, 1999.
16. Tsai, J.-Z., Will, J. A., Hubbard-Van Stelle, S., Cao, H., Tungjitkusolmun, S., Cho, Y. B., Haemmerich, D., Vorperian, V. R., and Webster, J. G., "In-Vivo Measurement of Swine Myocardial Resistivity," *IEEE Transactions on Biomedical Engineering*, vol. 49, no. 5, pp. 472-483, 2002.
17. Songer, J E, "Tissue Ischemia Monitoring Using Impedance Spectroscopy: Clinical Evaluation." Master of Science Worcester Polytechnic University, 2001.
18. Warren, M, "Electrical Impedance of Normal and Ischemic Myocardium. Role on the Genesis of ST Segment changes and Ventricular Arrhythmias." Ph.D. Thesis Universitat Autònoma de Barcelona, 1999.
19. Cinca, J., Warren, M., Carreño, A., Tresànceh, M., Armadans, L., Gómez, P., and Soler-Soler, J., "Changes in Myocardial Electrical Impedance Induced by Coronary Artery Occlusion in Pigs With and Without Preconditioning, Correlation With Local ST-Segment Potential and Ventricular Arrhythmias," *Circulation*, vol. 96, no. 9, pp. 3079-3086, 1997.
20. Bragos, R., Riu, J. P., Warren, M., Tresànceh, M., Carreño, A., and Cinca, J. Changes in myocardial impedance spectrum during acute ischemia in the in-situ pig heart. 1996. Amsterdam. 18th Annual Conference of the IEEE Engineering in Medicine and Biology Society.
Ref Type: Conference Proceeding
21. Jenderka, K. V. and Gersing, E. Comparison of impedance and ultrasound spectroscopy in investigations of ischemia caused alterations in organ tissue. 2, 855-856. 1996. Amsterdam. 18th Annual International Conference of the IEEE Engineering in Medicine and Biology Society.
Ref Type: Conference Proceeding
22. Gersing, E., Hofmann, B., Kehrer, G., and Pottel, R., "Modelling based on tissue structure: the example of porcine liver," *Innov.Tech.Biol.Med.*, vol. 16, no. 6, pp. 671-678, 1995.
23. Osypka, M. and Gersing, E., "Tissue impedance spectra and the appropriate frequencies for EIT," *Physiol Meas.*, vol. 16, no. 3 Suppl A, pp. A49-A55, Aug.1995.
24. Fallert, M. A., Mirotznik, M. S., Downing, S. W., Savage, E. B., Foster, K. R., Josephson, M. E., and Bogen, D. K., "Myocardial electrical impedance mapping of ischemic sheep hearts and healing aneurysms," *Circulation*, vol. 87, no. 1, pp. 199-207, 1993.
25. Kléber, A. G., Riegger, C. B., and Janse, M. J., "Electrical uncoupling and increase of extracellular resistance after induction of ischemia in isolated, arterially perfused rabbit papillary muscle," *Circulation Research*, vol. 61, no. 2, pp. 271-279, 1987.
26. Ellenby, M. I., Small, K. W., Wells, R. M., Hoyt, D. J., and Lowe, J. E., "On-line Detection of Reversible Myocardial Ischemic Injury by Measurement of Myocardial Electrical Impedance," *The Annals of Thoracic Surgery*, vol. 44 pp. 587-597, 1987.
27. Sola, A., Palacios, L., López-Martí, J., Ivorra, A., Noguera, N., Gómez, R., Villa, R., Aguiló, J., and Hotter, G., "Multiparametric monitoring of ischemia-reperfusion in rat kidney: effect of ischemic preconditioning," *Transplantation*, vol. 75, no. 6, pp. 744-749, Mar.2003.

28. Yamada, T., Hirose, H., Mori, Y., Onitsuka, A., Hayashi, M., Senga, S., Futamura, N., Sakamoto, K., Sago, T., Takagi, H., Yasumura, M., and Iwata, H., "Dielectric Spectrogram for Evaluating Ischemic Microstructural Changes of the Liver in Simple Cold Preservation," *Surgery Today*, vol. 32 pp. 1058-1063, 2002.
29. Haemmerich, D., Ozkan, O. R., Tsai, J. Z., Staelin, S. T., Tungjitkusolmun, S., Mahvi, D. M., and Webster, J. G., "Changes in electrical resistivity of swine liver after occlusion and postmortem," *Med.Biol.Eng.Comput.*, vol. 40 pp. 29-33, 2002.
30. Raicu, V., Saibara, T., and Irimajiri, A., "Multifrequency method for dielectric monitoring of cold-preserved organs," *Phys.Med.Biol.*, vol. 45 pp. 1397-1407, 2000.
31. Gersing, E., "Impedance spectroscopy on living tissue for determination of the state of organs," *Bioelectrochemistry and Bioenergetics*, vol. 45 pp. 145-149, 1998.
32. Ishikawa, M., Hirose, H., Sasaki, E., Bando, M., Mori, Y., and Murukawa, S., "Evaluation of myocardial viability during simple cold storage with the use of electrical properties in broad frequencies," *The Journal of Heart and Lung Transplantation*, vol. 15, no. 10, pp. 1005-1011, 1996.
33. Foucarde, C., Barbier, M., Perrin, P., Chigner de Alcantara, E., and Descotes, J., "Impédance tissulaire, Détermination de la viabilité du rein conservé en hypothermie," *La Nouvelle Presse médicale*, vol. 2, no. 13, pp. 837-838, 1973.
34. Harms, J., Schneider, A., Baumgartner, M., Henke, J., and Busch, R., "Diagnosing acute liver graft rejection: experimental application of an implantable telemetric impedance device in native and transplanted porcine livers," *Biosensors & Bioelectronics*, vol. 16 pp. 169-177, 2001.
35. Konishi, Y., Morimoto, T., Kinouchi, Y., Iritani, T., and Monden, Y., "Electrical properties of extracted rat liver tissue," *Research in Experimental Medicine*, vol. 195 pp. 183-192, 1995.
36. Gebhard, M. M., Gersing, E., Brockhoff, C. J., Schanabel, A., and Bretschneider, "Impedance spectroscopy: a method for surveillance of ischemia tolerance of the heart," *Thorac.cardiovasc.Surgeon*, vol. 35 pp. 26-32, 1987.
37. Garrido, H., Sueio, J., Rivas, J., Vilches, J., Romero, J. M., and Garrido, F., "Bioelectrical Tissue Resistance during Various Methods of Myocardial Preservation," *The Annals of Thoracic Surgery*, vol. 36, no. 2, pp. 143-151, 1983.
38. Pfitzmann, R., Müller, J., Grauhan, O., and Hetzer, R., "Intramyocardial impedance measurements for diagnosis of acute cardiac allograft rejection," *The Annals of Thoracic Surgery*, vol. 70 pp. 527-532, 2000.
39. Grauhan, O., Müller, J., Knosalla, C., Cohnert, T., Siniawski, H., Volk, H. D., Fietze, E., Kupetz, W., and Hetzer, R., "Electric myocardial impedance registration in humoral rejection after heart transplantation," *The Journal of Heart and Lung Transplantation*, vol. 15, no. 2, pp. 136-143, 1996.
40. Caduff, A., Hirt, E., Feldman, Y., Ali, Z., and Heinemann, L., "First human experiments with a novel non-invasive, non-optical continuous glucose monitoring system," *Biosensors & Bioelectronics*, vol. 19 pp. 209-217, 2003.
41. Schwan, H. P., "Electrical properties of tissue and cell suspensions," in Lawrence, J. H. and Tobias, C. A. (eds.) *Advances in Biological and Medical Physics* New York: Academic Press, 1957.

42. Foster, K. R. and Schwan, H. P., "Dielectric properties of tissues and biological materials: a critical review," *CRC Critical Reviews in Biomedical Engineering*, vol. 17 pp. 25-104, 1989.
43. Pethig, R., "Dielectric Properties of Biological Materials: Biophysical and Medical Applications," *IEEE Transactions on Electrical Insulation*, vol. EI-19, no. 5, pp. 453-474, 1984.
44. Gersing, E., "Monitoring temperature-induced changes in tissue during hyperthermia by impedance methods," *Annals of the New York Academy of Sciences*, vol. 873 pp. 13-20, 1999.
45. Casas, O., Bragos, R., Riu, J. P., Rosell, J., Tresànceh, M., Warren, M., Rodriguez-Sinovas, A., Carreño, A., and Cinca, J., "In Vivo and In Situ Ischemic Tissue Characterization Using Electrical Impedance Spectroscopy," in Riu, J. P., Rosell, J., Bragos, R., and Casas, O. (eds.) *Electrical Bioimpedance Methods: Applications to Medicine and Biotechnology* New York: The New York Academy of Sciences, 1999, pp. 51-58.
46. McAdams, E. T., Jossinet, J., and Lackermeier, A., "Modelling the 'Constant Phase Angle' behaviour of biological tissues: potential pitfalls," *Innov.Tech.Biol.Med.*, vol. 16, no. 6, pp. 662-670, 1995.
47. Flores, J., DiBona, D. R., Beck, C. H., and Leaf, A., "The role of cell swelling in ischemic renal damage and the protective effect of hypertonic solute," *J Clin Invest*, vol. 51, no. 1, pp. 118-126, 1972.
48. Groot, J R de, "Genesis of life-threatening ventricular arrhythmias during the delayed phase of acute myocardial ischemia. Role of cellular electrical coupling and myocardial heterogeneities." PhD Thesis University of Amsterdam, 2001.
49. Genescà, M., Ivorra, A., Sola, A., Palacios, L., Villa, R., and Hotter, G. Electrical bio-impedance monitoring of rat kidneys during cold preservation by employing a silicon probe. 127-130. 2004. Gdansk, Poland. Proceedings from the XII International Conference on Electrical Bio-Impedance (ICEBI). 20-6-0004.
Ref Type: Conference Proceeding
50. Ivorra, A., Villa, R., Genescà, M., Sola, A., Hotter, G., and Palacios, L. Medidas multifrecuenciales de bioimpedancia con una sonda miniaturizada de silicio. 219-222. 27-11-2002. Zaragoza, Spain. XX Congreso Anual de la Sociedad Española de Ingeniería Biomédica. 27-11-2002.
Ref Type: Conference Proceeding
51. Geddes, L. A., *Electrodes and the measurement of bioelectric events* New York: Wiley-Interscience, 1979.
52. Geddes, L. A. Who introduced the tetrapolar method for measuring resistance and impedance? *IEEE Engineering in Medicine and Biology Magazine* 15[5], 133-134. 1996.
Ref Type: Magazine Article
53. Pallás-Areny, R. and Webster, J. G., "AC instrumentation amplifier for bioimpedance measurements," *IEEE Transactions on Biomedical Engineering*, vol. 40, no. 8, pp. 830-833, Aug.1993.
54. Kinouchi, Y., Iritani, T., Morimoto, T., and Ohyama, S., "Fast in vivo measurements of local tissue impedances using needle electrodes," *Med.Biol.Eng.Comput.*, vol. 35 pp. 486-492, 1997.
55. Robillard, P. N. and Poussart, D., "Spatial Resolution of Four Electrode Array," *IEEE Transactions on Biomedical Engineering*, vol. 26, no. 8, pp. 465-470, 1979.

56. Steendijk, P., Mur, G., Van Der Velde, E. T., and Baan, J., "The Four-Electrode Resistivity Technique in Anisotropic Media: Theoretical Analysis and Application on Miocardial Tissue *in Vivo*," *IEEE Transactions on Biomedical Engineering*, vol. 40, no. 11, pp. 1138-1148, 1993.
57. Ivorra, A., Gómez, R., Noguera, N., Villa, R., Sola, A., Palacios, L., Hotter, G., and Aguiló, J., "Minimally invasive silicon probe for electrical impedance measurements in small animals," *Biosensors & Bioelectronics*, vol. 19, no. 4, pp. 391-399, 2003.

